

IMPROVED DISTANCE BASED UPGRIDDING FOR HIGH RESOLUTION
GEOLOGIC MODELS

A Thesis

by

IMROJ SYED

Submitted to the Office of Graduate and Professional Studies of
Texas A&M University
in partial fulfillment of the requirements for the degree of

MASTER OF SCIENCE

Chair of Committee,	Michael J. King
Committee Members,	Eduardo Gildin
	Art Donovan
Head of Department,	Jeff Spath

August 2020

Major Subject: Petroleum Engineering

Copyright 2020 Imroj Syed

ABSTRACT

Strong heterogeneities in properties characterize subsurface reservoirs and the encapsulation of these properties play an important role in optimizing the trade-off between preservation of geologic heterogeneity and reservoir simulation cost efficiency. The motivation of upgridding and upscaling high resolution geologic models is to develop practical and relatively low-resolution grids that are cost effective to run flow simulations whilst preserving as much reservoir heterogeneity as possible.

Upgridding high-resolution geologic models to considerably lower-resolution simulation models has always been extremely challenging for reservoir modeling and flow simulation, owing to the high heterogeneity and the complex controls on the porosity and permeability. In the past decades, development of high-resolution geologic models incorporated inclusion of greater detail in order to capture the spatial distribution of heterogeneity in rock properties, which affected oil and gas recovery. Orders of magnitude of $10^7 - 10^9$ cells are often encountered for geologic grids. Such high orders of magnitude are too expensive for routine flow simulation computations. Consequently, we develop and apply different upgridding algorithms applied across multiple reservoirs with varied distribution of heterogeneity and aim to maintain the best trade-off between preservation of information and minimization of cost.

In order to develop an optimized upgridding approach, various factors of the models have been taken into consideration. Combination of those factors lead to different choices in how we assess the reservoir heterogeneity that form the building blocks of different

upgridding approaches. We develop and apply a variety of upgridding schemes (layer designs) for diverse geologic models and observe how the different algorithms behave.

The current study of multiple algorithms and their upgridding performance for various models has led to the development of a **novel distance-based upgridding technique** which appears to be more effective in terms of characterizing the physical model properties. This approach is developed and applied in the current study.

DEDICATION

To my parents and my loved one for their love, blessings, encouragement and support always. To the Almighty, Allah for bestowing graciousness and mercy during the progress and completion of my research work.

ACKNOWLEDGEMENTS

I would like to express my deepest gratitude for my graduate advisor Dr. Michael J. King for his constant support, encouragement, patience, motivation, inspiration, academic guidance and financial support throughout my research. His time and efforts contributed to this research are very valuable and helped me all the time in completion of this research and thesis.

I would like to thank Dr. Eduardo Gildin and Dr. Art Donovan for imparting their time and efforts in helpful suggestions and comments towards this dissertation. Their presence in my research committee are gratefully acknowledged.

I would also like to thank all my colleagues in and out of my research group who have helped me with their insightful ideas and discussions.

I would take this opportunity to acknowledge the financial support from members of the Joint Industry Project (JIP) with the Model Calibration and Efficient Reservoir Imaging (MCERI) research group. The computer labs and IT facilities provided by the Department of Petroleum Engineering; Texas A&M University have helped me achieve completion of my research successfully.

Also, I would like to acknowledge Roxar and Schlumberger for being the user of their reservoir modeling and simulation software, namely RMS, ECLIPSE and Petrel.

CONTRIBUTORS AND FUNDING SOURCES

Contributors and Funding Sources

This research work was supervised by a research committee consisting of Professor Dr. Michael J. King [advisor], Professor Dr. Eduardo Gildin of the Department of Petroleum Engineering and Professor Dr. Art Donovan, of the Department of Geology and Geophysics.

The data analyzed for my research includes Amellago Carbonate Model, which was provided by Dr. Sebastian Geiger, head of the Carbonate Reservoir Group at the Heriott Watt University. Also, once again Roxar and Schlumberger are acknowledged for being the user of their modeling software.

All other work conducted for the thesis involved data sets provided by my research committee.

Graduate study was supported by a Graduate Research Assistantship from Texas A&M University, in collaboration with the Model Calibration and Efficient Reservoir Imaging (MCERI) led by Dr. Akhil Datta-Gupta and the Energi Simulation research group.

NOMENCLATURE

k_x, k_y, k_z	Permeability along x-, y- and z-direction respectively
k_H, k_V	Horizontal and Vertical Permeability respectively
ϕ	Porosity
ΔP	Pressure Differential
A_i	Area of Cross-Section of the i th cell in a grid
$\Delta x, \Delta y, \Delta z$	x, y and z dimensions of a cell in the grid
T_x, T_y, T_z	Transmissibilities along x-, y- and z-directions respectively
B	Between Cell Heterogeneity
W	Within Cell Heterogeneity
V	Velocity Error Measure
S	Slowness Error Measure
VS	Combination of Velocity and Slowness Error Measures in SWIFT
VxS	Combination of Velocity and Slowness Error Measures in Distance Based Upgridding
H	Total Heterogeneity
P_{ijk}	Cell Property
\bar{P}_{ijk}	Averaged Cell Property
P_{ijk}^C	Coarsened Cell Property
$\delta B, \delta W$	Change in Between and Within Cell Heterogeneity respectively

TABLE OF CONTENTS

	Page
ABSTRACT	ii
DEDICATION	iv
ACKNOWLEDGEMENTS	v
CONTRIBUTORS AND FUNDING SOURCES.....	vi
Contributors and Funding Sources	vi
NOMENCLATURE.....	vii
TABLE OF CONTENTS	viii
LIST OF FIGURES.....	x
LIST OF TABLES	xiii
CHAPTER I INTRODUCTION	1
3D Geologic models.....	2
SPE10 (60x220x85)	4
Amellago (79x80x1099)	6
Upgridding and Upscaling	12
Motivation: Issues with Existing Upgridding Techniques.....	22
CHAPTER II LITERATURE REVIEW	27
Testerman (1962)	28
Durlflosky et al. (1996)	30
Li et al. (1996).....	31
Stern and Dawson (1999).....	32
Li and Beckner (2000).....	32
Fincham et al. (2004)	33
King et al. (2006)	33
Kim and Datta-Gupta (2009).....	34
Hosseini and Kelkar (2008) and (2010)	35
SWIFT (2012)	35

CHAPTER III IMPROVED UPGRIDDING TECHNIQUES	41
Improved Upgridding: Introduction of Cutoffs.....	41
Improved Upgridding: Choice of Weighting Factors	47
Improved Upgridding: Zonal Averaging and Zonal Upgridding	54
CHAPTER IV DISTANCE BASED UPGRIDDING.....	67
Theoretical Background	67
Novelty: How novel is this method?.....	68
Testing Distance Based Upgridding on SPE10.....	69
Testing Distance Based Upgridding on Amellago Model	73
CHAPTER V DISCUSSIONS	77
Advantages	77
Summary	79
CHAPTER VI CONCLUSIONS	80
REFERENCES.....	82

LIST OF FIGURES

	Page
Figure 1: Upgridding and Upscaling as a part of a Reservoir Modeling and Simulation Workflow (Roxar (2012))	2
Figure 2: Property Distribution for SPE10 Model. Histograms of (a) Porosity, (b) Horizontal Permeability, (c) Ratio of Horizontal Permeability and Porosity, (d) Ratio of Vertical and Horizontal Permeability	6
Figure 3: 3D Property Distributions for Amellago Carbonate Model, (a) Horizontal Permeability (k_H) Distribution, (b) Zones or Stratigraphic Units, (c) Environments of Deposition (EODs), (d) Facies Distribution	9
Figure 4: Property Distribution for Amellago Carbonate Model. Histograms of (a) Porosity, (b) Horizontal Permeability, (c) Ratio of Horizontal Permeability and Porosity, (d) Ratio of Vertical and Horizontal Permeability	10
Figure 5: Workflow of Upgridding: Layer Coarsening	13
Figure 6: Workflow of Upscaling: Choosing Section of Fine Scale Model as an Illustration of Property Averaging	15
Figure 7: Arithmetic Averaging Permeability Upscaling	16
Figure 8: Harmonic Averaging Permeability Upscaling	18
Figure 9: Two Cell Representation of Flow	19
Figure 10: Transmissibility Upscaling Along Horizontal Direction	20
Figure 11: Transmissibility Upscaling Along Vertical Direction	21
Figure 12: Upgridding Heterogeneity Plots for Amellago Carbonate Model	23
Figure 13: Layering Summary for SWIFT Coarsening for Amellago Carbonate Model	24
Figure 14: 2D Areal Map of Zonal Net Rock Volume, Average Porosity and Average Permeability	25
Figure 15: Chronology of Technical Advancements in Upgridding	27

Figure 16: Procedure for Layer Selection (Stern and Dawson (1999)).....	32
Figure 17: Frontal Velocity Variance used as Error Measure.....	34
Figure 18: Workflow of SWIFT.....	38
Figure 19: Upgridding Heterogeneity Plots for SPE10 Model along with the method of selection of Optimal Number of Layers: Maximum Area Method.....	39
Figure 20: Upgridding Heterogeneity Plots – Comparing effects of Cutoff for various error measures.....	47
Figure 21: Choice of Cutoff to be used for Comparison of Weighting Factors.....	49
Figure 22: Upgridding Heterogeneity Plots: Comparison of Weighting Factors.....	51
Figure 23: Effect of Weighting Factors: Optimal Layering Distribution of Amellago with No Cutoff.....	52
Figure 24: Effect of Weighting Factors: Optimal Layering Distribution of Amellago With Cutoff.....	52
Figure 25: Effect of Cutoffs + Weighting Factors: Optimal Layering Distribution of Amellago.....	53
Figure 26: Effect of Cutoffs + Weighting Factors: Heterogeneity Plot.....	53
Figure 27: Upgridding Heterogeneity Plot for Amellago: Column Averaging vs Zonal Averaging.....	55
Figure 28: Effect of Averaging on the Optimal Layering Distribution for Amellago.....	56
Figure 29: Layering Distribution of Amellago using Column Averaging Method.....	57
Figure 30: Optimal Layering Distribution of Amellago using Zonal Averaging Method.....	58
Figure 31: 2D Map View of Different Properties of Amellago Model (Liu, 2019)	60
Figure 32: Optimal Layering Distribution for Amellago: Comparison of Zonal Upgridding vs Other Methods.....	61

Figure 33: Upgridding Heterogeneity Plot for Amellago: Comparison of Zonal Averaging	62
Figure 34: Amellago Zonal Layer Design Heterogeneity Plot (Three Heterogeneity Measures) (Liu, 2019).....	63
Figure 35: Comparison of Optimal Layering Distribution for Amellago: Zonal Averaging vs. Zonal Upgridding	64
Figure 36: Amellago 3D Model: Well Locations for Flow Simulation	64
Figure 37: Total Production Flow Rates Comparison for Amellago	65
Figure 38: L2 Norm Errors for Well Rates for Amellago.....	65
Figure 39: SPE10 Layering Scheme	70
Figure 40: SPE10 Upgridding Heterogeneity Plot.....	70
Figure 41: SPE10 3D Model: Well Locations for Flow Simulation	71
Figure 42: SPE10 Single Phase: Cumulative Oil Production	72
Figure 43: SPE10 Single Phase: Field Flow Rate	72
Figure 44: SPE10 Single Phase: Field Flow Rate Errors	73
Figure 45: Amellago Layering Scheme	73
Figure 46 Amellago Upgridding Heterogeneity Plot	74
Figure 47: Amellago 3D Model: Well Locations for Flow Simulation	75
Figure 48 Amellago Simulation Results: Cumulative Oil Production.....	75
Figure 49 Amellago Simulation Results: Field Flow Rates.....	76
Figure 50 Amellago Simulation Results: Field Flow Rates Errors	76
Figure 51 Distance Based VxS Heterogeneity Plot Compared with SWIFT Heterogeneity Plots.....	77
Figure 52 Layering Scheme for Amellago model comparison: Distance Based VxS vs SWIFT algorithms.....	78

LIST OF TABLES

	Page
Table 1: Zonal Averaged Properties of the SPE10 Model	4
Table 2: 2D Areal Map of Average Porosity and Average Permeability of SPE10	5
Table 3 - Elements of Amellago Carbonate Model.....	7
Table 4 - Zonal Averaged Properties of the Amellago Carbonate Model.....	8
Table 5 - Choice of cutoff based on $\frac{k_H}{\phi}$ Distributions	42
Table 6 - SWIFT Layering Distribution for Amellago Carbonate Model	43
Table 7 - Comparison of Cutoffs in Distribution of Fine Layers into Coarse Layers	44
Table 8 - Effect of Cutoffs on the Optimal Number of Layers (Amellago).....	45
Table 9 - Porosity and Horizontal Permeability Distribution of Amellago	48
Table 10 - Effect of Averaging Method on Optimal Layer Count for Amellago	57

CHAPTER I

INTRODUCTION

Reservoir simulation and modeling encompasses an important domain of reservoir engineering. It is an important component of any modern reservoir management tool. Forecasting for hydrocarbon recovery and estimating reservoir performance for optimization purposes are some of the common tasks performed using this technology. However, this task of reservoir simulation often becomes cumbersome on the high-resolution geologic models prepared by the group of geologists and geophysicists. While greater information about the reservoir statics and dynamics are very important in understanding of the physical, chemical and thermodynamics of the subsurface resource, not all of it is necessary for simulation. Similarly, precise information about every single grid of a high-resolution geologic model may be inconvenient for the multitude of simulation processes necessary to be run repeatedly over the same model or piece of a model; the inconvenience being computational efficiency which in turn results in expense for any commercial process. Therefore, in order to make computation economic, we require to transform the high-resolution 3D geologic grid into a relatively low-resolution simulation grid. This transformation involves the process of “Upgridding” and “Upscaling”. Upgridding involves coarsening the high-resolution grid into the low-resolution grid by merging cells and layers. Once the coarsened grid has been designed, Upscaling is the process to populate the coarsened grid with the best average properties. A good upgridding and upscaling technique would preserve the most important flow characteristics of geologic models.

3D Geologic models

Geologic modeling involves creation of a geologic framework, followed by populating the framework by reservoir rock and fluid data, geothermal field, pressure field distributions. All these are built based on the structural model and in order to minimize uncertainty of the model, deterministic information is used as much as possible. Unlike other more basic models like proxy models or mass balance models, these 3D geologic models represent and predict the reservoir energy and fluid front propagation and sweep. However, they are slow to build and update owing to the amount of details involved in their construction

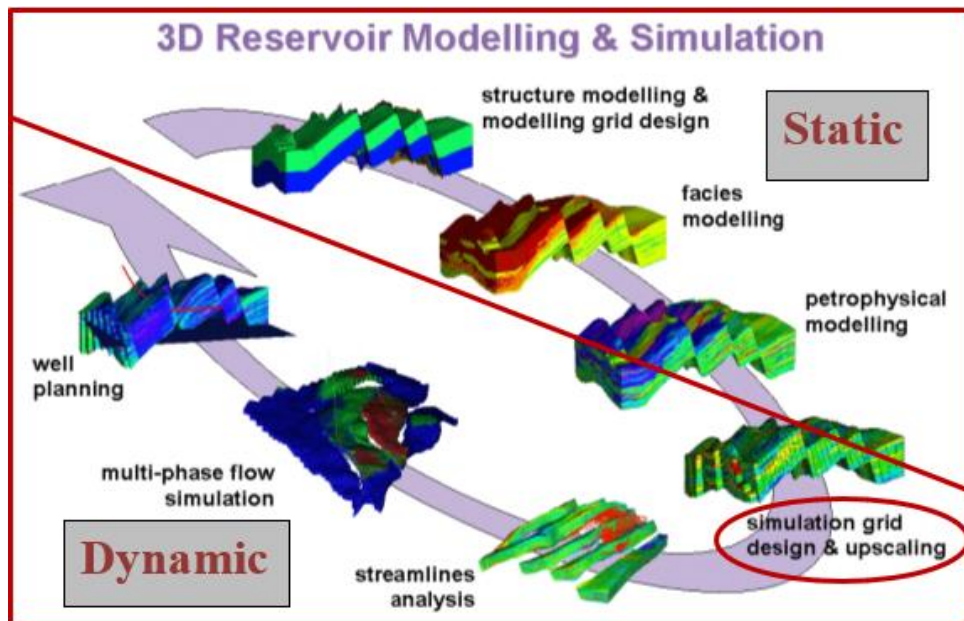


Figure 1: Upgridding and Upscaling as a part of a Reservoir Modeling and Simulation Workflow (Roxar (2012))

Figure 1 is a pictorial representation of the workflow for any detailed 3D reservoir modeling and simulation. This workflow begins with the high resolution static geologic

model, incorporating structural grid design of multimillion cells, facies modelling and petrophysical modelling. Typically, the number of cells in this geologic model varies somewhat between 10 to 100 million cells, thereby providing highly detailed description of the reservoir. Simulation models are the simpler dynamic models, the simplification performed in order to save computational time while running several simulations on the model. They are typically one or two orders of magnitude simpler. The geologic model is generally built by integrating both the well log data and seismic data using geostatistical tools. Transformation from the well log scale to the scale of the blocked well for the geologic model involves a 1D upscaling calculation.

The transformation of the multi-million celled geologic grid into a fairly low-resolution simulation grid is where Upgridding and Upscaling operate. However, a finer aspect to areal coarsening in Upgridding is 'Adaptive Gridding'. We would like to preserve high resolution in the cells around the wells, however deeper into the model we may choose to coarsen with a higher coarsening ratio. This process of areal upgridding would, hence be chosen to be performed at a later stage than normal Upgridding and Upscaling, i.e. after the well planning is done and we have the exact well locations.

The 3D geologic models used for testing purposes for my research include:

- SPE10 (60x220x85 cells): A sandstone reservoir model.
- Amellago (79x80x1099 cells): A carbonate ramp outcrop model.

Our research group has previously tested multiple sandstone reservoir models and performed upgridding on them. However, this is the first time to test our existing

upgridding algorithms on a carbonate mode. We observed anomalous results and thereby began probing into the underlying physics of our algorithms.

The above two geologic models will be characterized here in the following section.

SPE10 (60x220x85)

SPE10 is a simple sandstone geologic model. It has simple geometry, with no top surfaces or faults. It is described on a regular cartesian grid. The model dimensions are 60 x 220 x 85 (1,122,000 cells).

The model consists of a part of a Brent sequence and is characterized by two formations. The first in the top 35 layers represents the Tarbert formation which is a representation of a pro-grading near shore environment. It is a low contrast, high permeability stratified sand structure. The second geologic unit is the bottom 50 layers which is a part of the Upper Ness sequence and represents fluvial environment. It consists of high permeability channels embedded in a background of low permeability. SPE10 is particularly challenging for many simulators because of its strong variations in heterogeneity in permeability. Table 1 represents the zonal/stratigraphic average properties of SPE10 model.

Table 1: Zonal Averaged Properties of the SPE10 Model

Stratigraphic Unit	Layers	Layer Count	Average Thickness [ft]	Average Porosity [%]	k_H [mD]	k_V [mD]	Pore Volume (PV) [MM ft³]
Tarbert	1 - 35	35	70	19.08	356.49	94.09	35.26
Upper Ness	36-85	50	100	15.64	354.96	33.47	41.3

Table 2 below shows a better view of the difference in the flow pattern of the two stratigraphic units.

Table 2: 2D Areal Map of Average Porosity and Average Permeability of SPE10

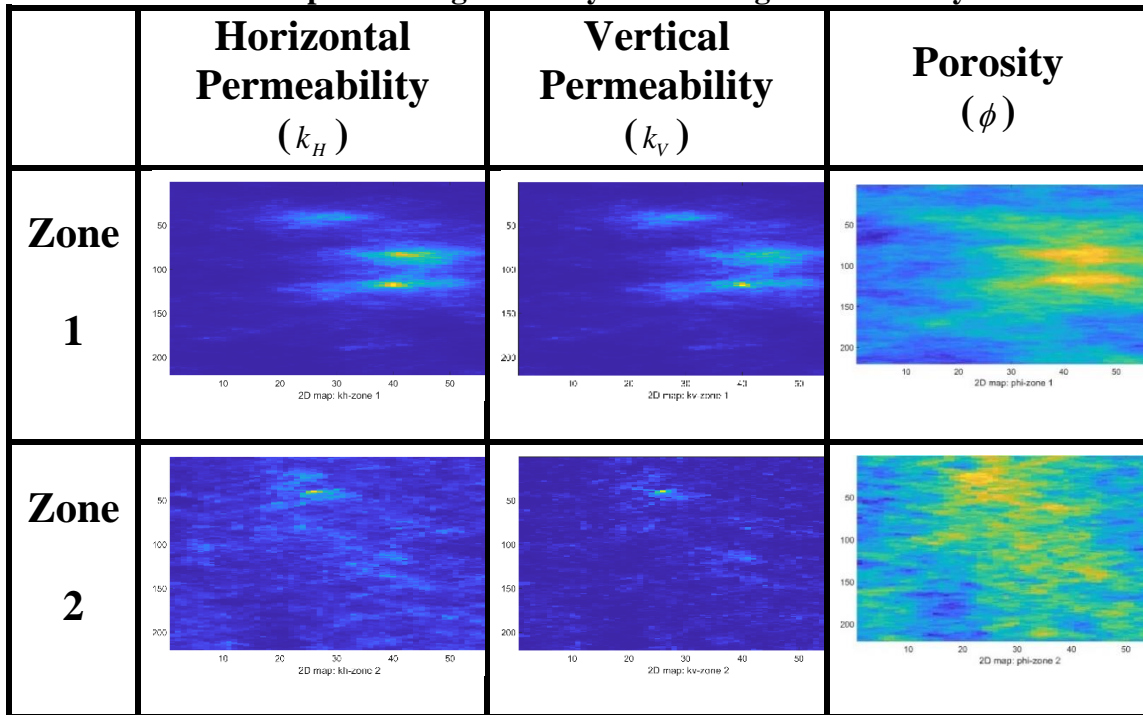


Figure 2 is a pictorial representation of the property distributions of SPE10: porosity, horizontal permeability, ratio of horizontal permeability and porosity, ratio of horizontal and vertical permeability. In all cases, we notice the bi-modal distribution, owing to the presence of the two distinct geologic units.

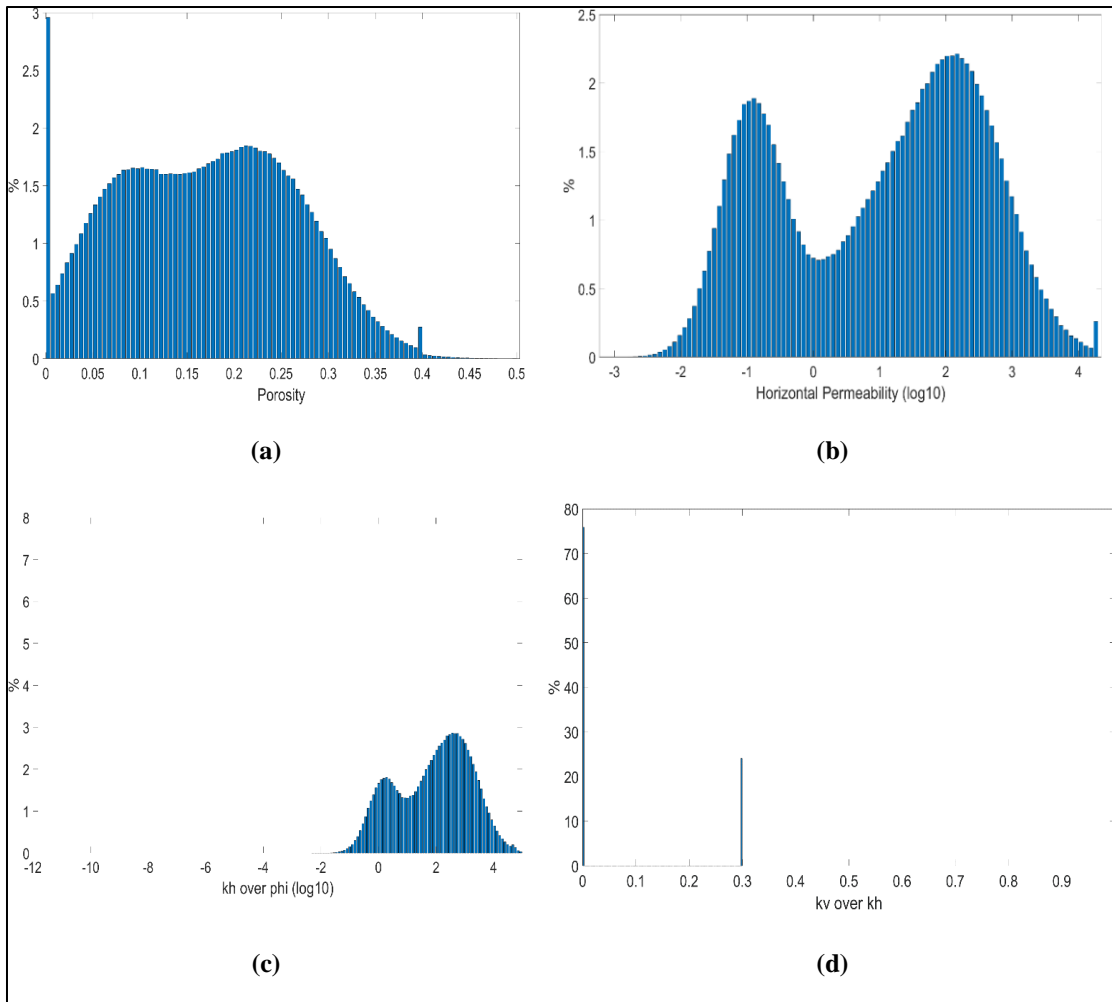


Figure 2: Property Distribution for SPE10 Model. Histograms of (a) Porosity, (b) Horizontal Permeability, (c) Ratio of Horizontal Permeability and Porosity, (d) Ratio of Vertical and Horizontal Permeability

Amellago (79x80x1099)

A greater part of our motivation for improvement of upgridding techniques arose while dealing with coarsening of Amellago model. Hence, it is important to know the features of this model that make coarsening a challenge. We would go through a detailed description of the Amellago model, to give the reader an in-depth understanding of the

astronomical variation in spatial distribution of heterogeneity in the model and the reason why we encountered issues with our existing upgridding algorithms.

Amellago, a Jurassic age carbonate ramp outcrop, is in the High Atlas Mountains of Morocco. Developed by ExxonMobil, this model has been provided for research by Dr. Sebastian Geiger from Heriott-Watt University.

This model has been developed with the following elements tabulated in Table 3.

Table 3 - Elements of Amellago Carbonate Model

Number of cells = 6,945,680 (79x80x1099)			
Number of Active cells = 6,480,803 cells (93.31%)			
Average Cell Size = 15.19 m x 15.49 m x 21 cm			
Stratigraphic Units	Faults	Environments of Deposition	Facies Associations
8	5	8	14
Horizontal Permeability: $k_H(\phi)$ uniform transform per facies, $k_x = k_y = k_H$			
Vertical Permeability: $\frac{k_v}{k_H}$ ratio values are uniform per facies			

The Depositional Environments are geostatistical distributions controlled by the stratigraphic units. The Facies are also geostatistical distributions controlled by the depositional environments. Porosity is a geostatistical distribution too and controlled by facies with additional diagenetic effects.

Table 4 - Zonal Averaged Properties of the Amellago Carbonate Model

Stratigraphic Unit	Layers	Layer Count	Average Thickness [m]	Average Porosity [%]	k_H [mD]	k_V [mD]	Pore Volume (PV) [MM m3]
ISO-s4	1 - 158	158	32.46	5.35	139.27	111.29	2.62
ISO-hg4	159 - 343	185	38.01	4.54	19.52	5.5	1.90
ISO-hg3	344 - 408	65	13.35	12.92	380.71	64.07	0.58
ISO-hg1	409 - 620	212	43.55	3.96	114.72	93.28	3.13
ISO-s3	621 - 688	68	13.97	12.35	52.12	41.2	0.93
ISO-s2	689 - 741	53	10.88	15.84	127.46	103.98	0.74
ISO-s1	742 - 804	63	12.94	13.33	198.68	163.12	1.50
ISO-base	805 - 1099	295	60.61	2.84	99.07	79.37	3.71
Total	1 - 1099	1099	225.81	6.37	115.16	77.4	15.10

Table 4 lists the zonal averaged properties of the Amellago model. This table helps to observe the variability in the flow quality of adjacent zones. For instance, zones highlighted in red and blue: ISO-hg4 and ISO-hg1 are adjacent and have a very high difference in average permeabilities.

Figure 3 represents the 3D images of the Amellago geologic model depicting property distribution, stratigraphic units, environments of deposition and facies associations.

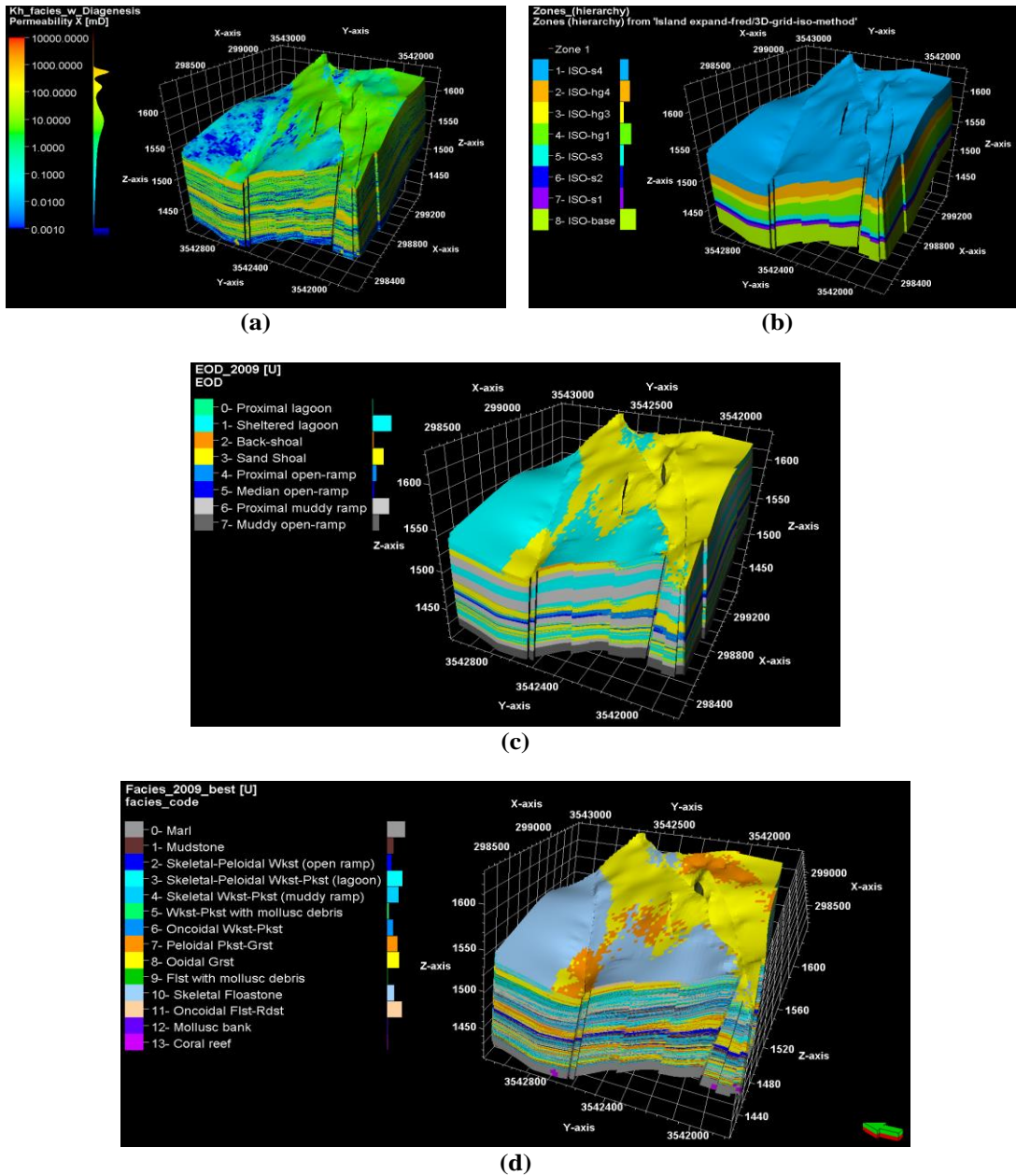


Figure 3: 3D Property Distributions for Amellago Carbonate Model, (a) Horizontal Permeability (k_H) Distribution, (b) Zones or Stratigraphic Units, (c) Environments of Deposition (EODs), (d) Facies Distribution

Referring to Table 4, we already noticed how the different zones are stacked against each other with widely varied properties. The zones colored in red and blue were two adjacent zones with porosity and horizontal permeability values varying over orders of magnitude. Later in this dissertation, we have used measures to maintain this heterogeneity distribution in our coarsened models too. This table would re-appear multiple times in the document, with additional information about how the coarsened schemes behave for each zone.

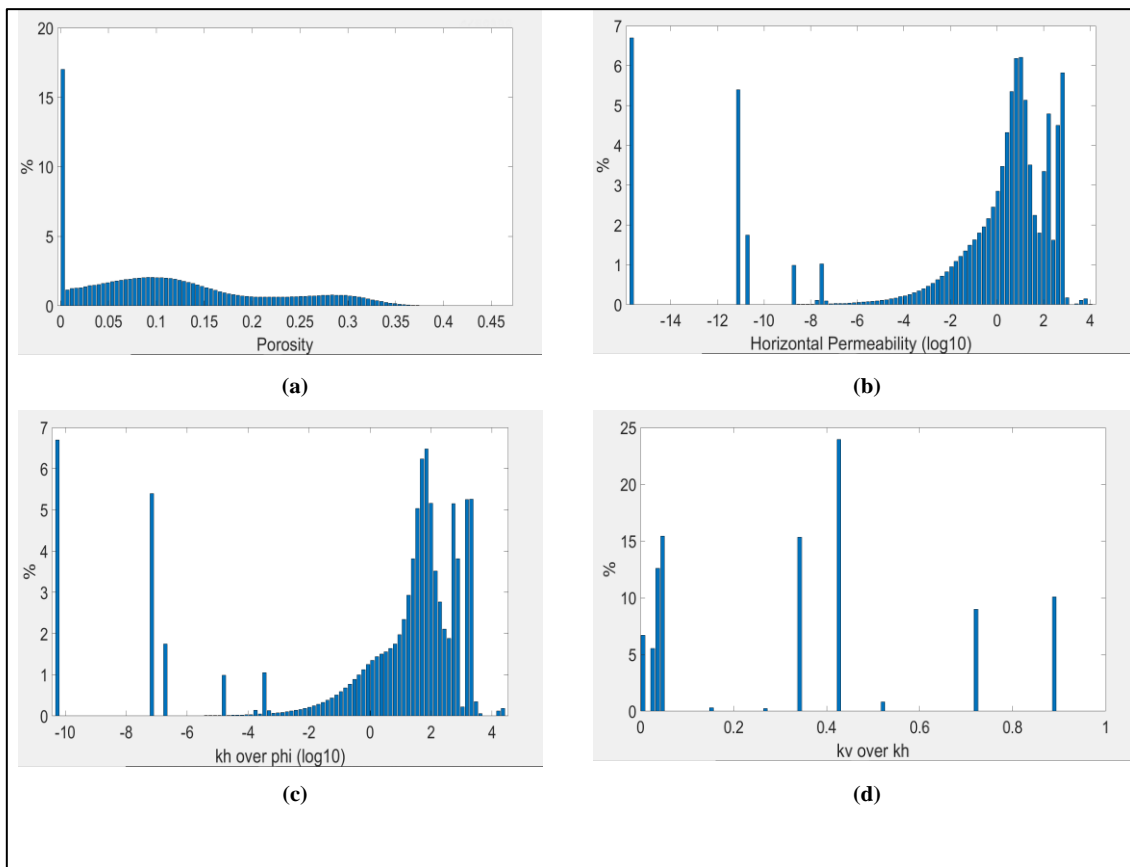


Figure 4: Property Distribution for Amellago Carbonate Model. Histograms of (a) Porosity, (b) Horizontal Permeability, (c) Ratio of Horizontal Permeability and Porosity, (d) Ratio of Vertical and Horizontal Permeability

The Amellago model has been constructed based on the elements of Table 3. The structural description of the model is fairly simple, comprising of 5 faults that have sufficient throw to juxtapose differing layers of the reservoir, thereby rendering formation of 3 main fault blocks. However, the faults do not intersect to form totally isolated fault blocks. The internal reservoir architecture comprising of 8 stratigraphic units is based upon the 8 depositional environments, which control the facies associations and the spatial distribution of the 14 facies. The spatial distribution of the permeability is obtained from the porosity-permeability correlations and the $\frac{k_V}{k_H}$ ratio, which are specified for each facies.

Figure 4 shows the statistics of the model properties. Owing to the facies-based modeling, all of these properties exhibit multi-modality. Although none of these cells in the model have been identified as non-net, it is noticed that there are some extremely low permeability cells. Permeability values have a broad distribution over many orders of magnitude. The smoothness and width of the permeability distribution indicates that identifying a non-net threshold is very problematic. The cell $\frac{k_V}{k_H}$ ratio can also be very low (as low as ~0.05) indicating vertical flow baffles locally existent within the facies. At the reservoir scale, vertical flow can be expected to be controlled by the horizontal continuity of the low permeability facies, and not by the cell $\frac{k_V}{k_H}$ ratio. Finally, we also include the $\frac{k_H}{\phi}$ distribution (also called as ‘Velocity’) which controls both the speed of

the multiphase horizontal frontal advance through the interstitial velocity, and the speed of the pressure propagation through the diffusivity.

By looking at these property statistics, our attempt was to depict that the Amellago model is highly heterogeneous. Very low values of horizontal permeability lead to extremely high values of slowness, which when used in heterogeneity variance calculations renders minor changes in the values of slowness. This leads to variance preserved to almost 100% for slowness to a very few layers.

Upgridding and Upscaling

Upgridding and Upscaling are the model coarsening techniques. They work in tandem. Upgridding involves coarsening the fine scale high-resolution geologic model into the low-resolution simulation model. This coarsening is achieved by vertically grouping multiple fine scale layers and/or areal grouping fine grid cells into coarse cells. In this dissertation, we would be focusing on the vertical coarsening, or in other words “Layer Grouping” for geologic models. Areal coarsening is generally dependent on the CPU requirements of the computer and 2x2 or 3x3 areal grid coarsening maybe chosen accordingly. However, recent researches are also being made on the unstructured gridding for complex reservoir geometries. Also, as mentioned before Areal coarsening is largely dependent on the well locations. However, that is out of the scope of this research paper and will not be discussed.

Let us discuss the premise of Upgridding.

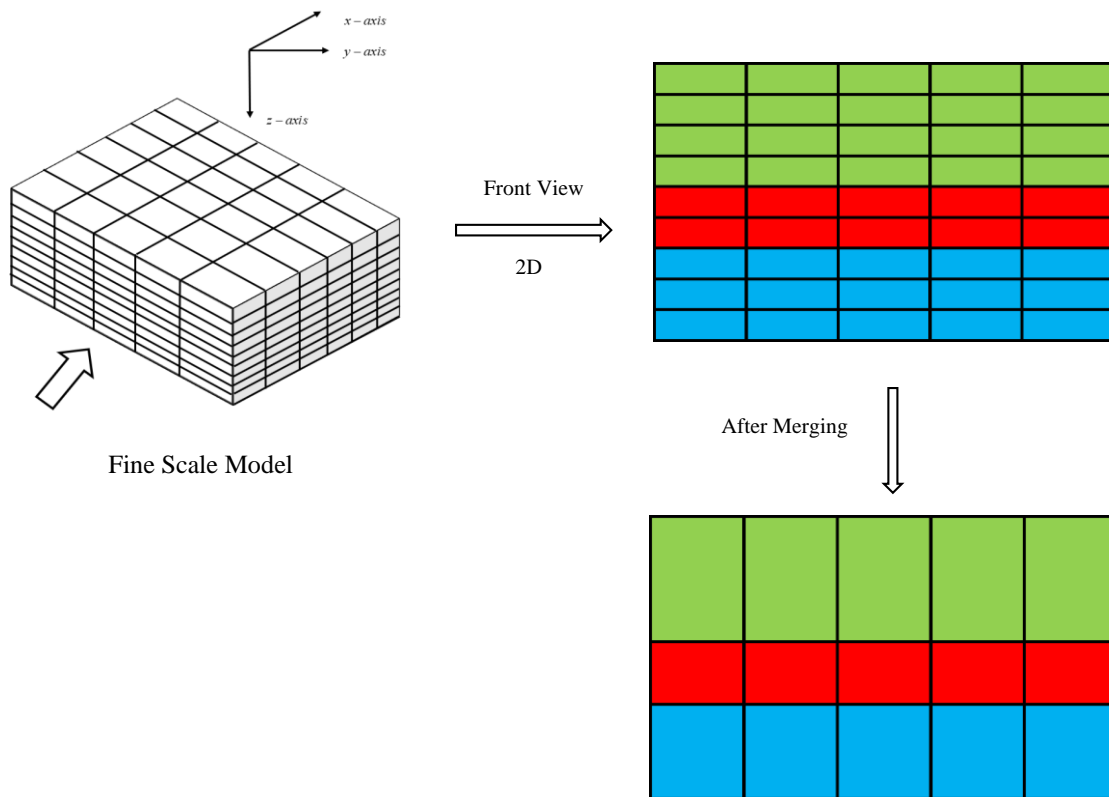


Figure 5: Workflow of Upgridding: Layer Coarsening

We start with the high-resolution geologic model and intend to group the fine scale layers in order to obtain a low resolution coarse scaled simulation model. In Figure 5, the fine scale model has 9 layers. The first 3 fine layers are chosen to group into 1 coarse layer, the next 2 fine layers into another coarsened layer and the last 3 fine layers are merged to the last layer of the coarsened model. The method of choosing which two or more adjacent layers to merge is a major domain of research. The chapter “Literature Review” will explain how the former researchers thought about various mechanisms to group layers.

The underlying mathematics and physics involved in the starting point of my research is also discussed in the last section “SWIFT (2012)” of the “Literature Review”. This dissertation discusses the steps to the development of an improved Distance-based upgridding technique and the corresponding results.

Next, we discuss about “Upscaling”. After the coarsened grid has been optimally prepared by the upgridding tool, we need to populate the coarsened grid with coarse scale properties. These coarsened properties are primitively often average of the fine scale properties. However, in order to preserve the fidelity of the reservoir, i.e. reservoir heterogeneity information, different advanced techniques of upscaling have been adopted. In this research thesis, we will NOT be developing any new “Upscaling” techniques. We will, however, mention and discuss the mechanics of the chosen upscaling methods and how they compare with the fine scale model.

We have chosen to explore two specific methods of “Upscaling”:

- “Permeability” based: static properties like permeabilities are averaged and then these averages are used to define the flow properties of the model
- “Transmissibility” based: transmissibilities are averaged maintaining the pressure equilibrium and solving for flow equations.

In all our cases in this dissertation, we would be performing $1 \times 1 \times N$ upscaling only, i.e. no areal upscaling would be performed. This makes certain calculations for horizontal property upscaling very easy. Since the main focus in this literature has been layer grouping, so would focus more on the Z-direction upscaling more.

We will formulate the mechanics of these methods and show how the corresponding results look like.

To begin with, let us use the same fine scale model that was shown for “Upgridding” in Figure 5.

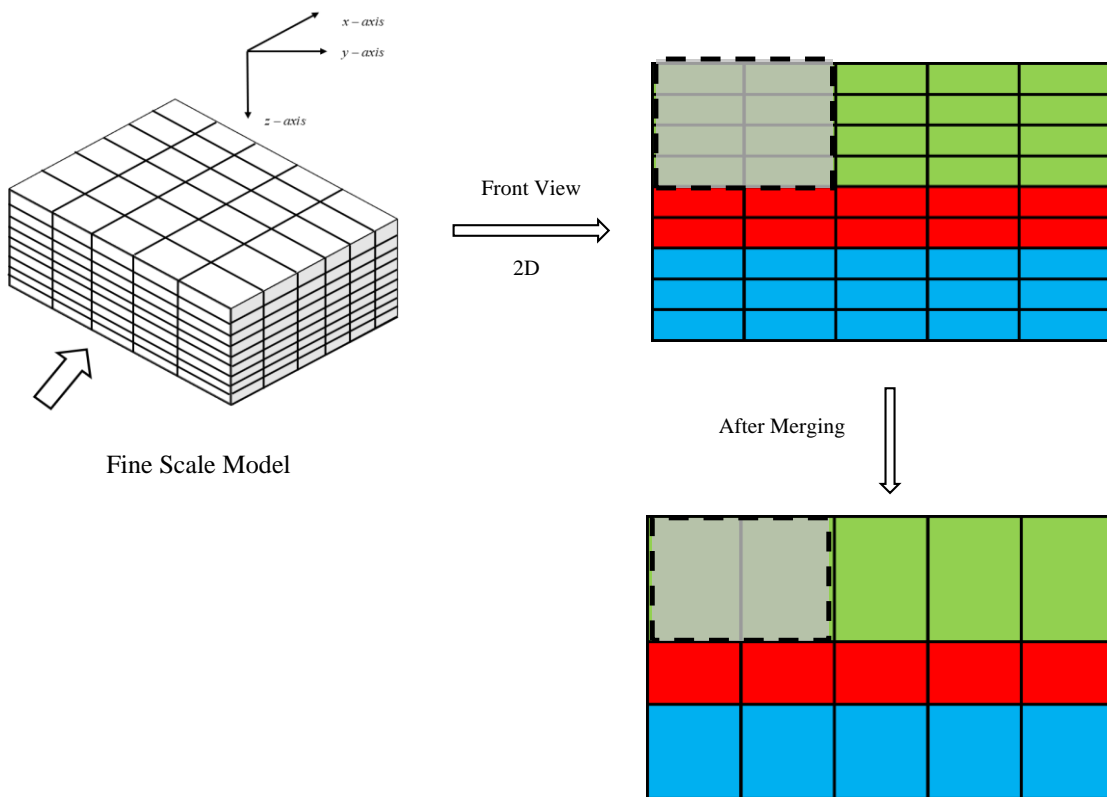


Figure 6: Workflow of Upscaling: Choosing Section of Fine Scale Model as an Illustration of Property Averaging

Let us choose the first two columns of the fine scale model as shown by the highlighted grid cells in Figure 6. First, we would go through the “Permeability” based upscaling.

- **Permeability Based Upscaling:** Horizontal and Vertical directional properties are handled differently. For horizontal properties, we upscale the permeabilities by the simple arithmetic average. This is illustrated in Figure 7. We establish a pressure boundary across the selected cells as shown by the vertical red broken lines.

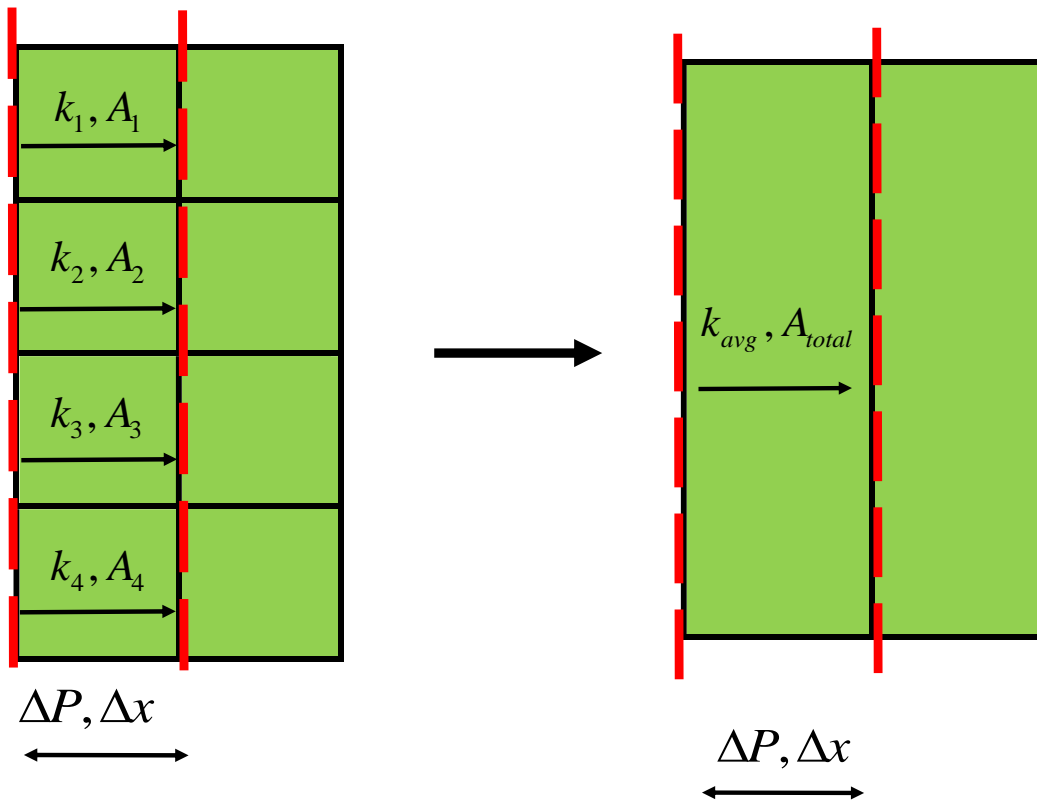


Figure 7: Arithmetic Averaging Permeability Upscaling

The expression for averaged permeability is:

$$k_{avg} = \frac{\sum_{i=1}^N k_i A_i}{\sum_{i=1}^N A_i} \dots\dots\dots (1)$$

Where,

k_i = permeability (mD)

A_i = cross sectional area (sq. ft.)

Now, we calculate the associated intercell transmissibility for the upscaled grid. Let us choose two adjacent coarse cells (indexed as i and $i+1$) and perform transmissibility calculations.

For X-transmissibility,

$$T_x = C \frac{\left[\frac{\Delta x_{i+1} (\Delta y_i \Delta z_i) + \Delta x_i (\Delta y_{i+1} \Delta z_{i+1})}{\Delta x_i + \Delta x_{i+1}} \right]}{\left(\frac{\Delta x_i}{k_{x_i}} + \frac{\Delta x_{i+1}}{k_{x_{i+1}}} \right) / 2} \dots\dots\dots (2)$$

Where, $\Delta x, \Delta y, \Delta z$ are cell dimensions in the x-, y- and z- directions

C = unit conversion constant = 0.00112712 (field units) or, 0.00852702 (metric units)

For Y-transmissibility,

$$T_y = C \frac{\left[\frac{\Delta y_{i+1} (\Delta x_i \Delta z_i) + \Delta y_i (\Delta x_{i+1} \Delta z_{i+1})}{\Delta y_i + \Delta y_{i+1}} \right]}{\left(\frac{\Delta y_i}{k_{y_i}} + \frac{\Delta y_{i+1}}{k_{y_{i+1}}} \right) / 2} \dots\dots\dots (3)$$

For estimation of vertical permeability upscaling, we use harmonic average. This is illustrated in the Figure 8. Here, we establish pressure boundaries across the selected cells as shown by the horizontal red broken lines. The method of choosing the pressure boundary is finding the $\sum \Delta z$ from the face between the coarse blocks corresponding to 50% of $\sum \Delta z$ for that set of fine cells comprising the coarse block. In this case, the pressure boundaries are set along the black broken lines.

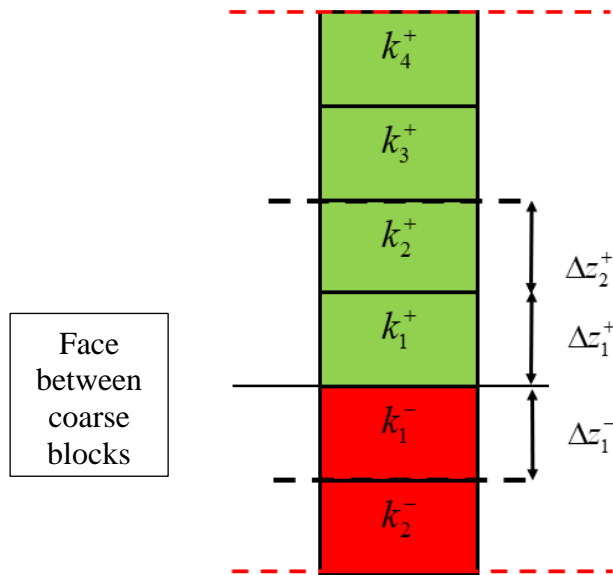


Figure 8: Harmonic Averaging Permeability Upscaling

The expression for averaged permeability is:

$$k_{avg} = \frac{\sum_{i=1}^N \Delta z_i}{\sum_{i=1}^N \frac{\Delta z_i}{k_i}} \dots\dots\dots (4)$$

Where,

Δz_i = thickness of each layer (ft)

Now, calculation of the transmissibility is as follows:

For Z-transmissibility,

$$T_z = C \left[\frac{\Delta z_{i+1} (\Delta x_i \Delta y_i) + \Delta z_i (\Delta x_{i+1} \Delta y_{i+1})}{\Delta z_i + \Delta z_{i+1}} \right] \dots\dots\dots (5)$$

$$\left(\frac{\Delta z_i}{k_{z_i}} + \frac{\Delta z_{i+1}}{k_{z_{i+1}}} \right)$$

$$2$$

- **Transmissibility Based Upscaling:** Here, instead of calculating the average permeability, we calculate the transmissibilities in the fine grid and then using pressure solver equations average the transmissibilities for the coarsened grid. This method has been established to capture better flow properties across models of different resolutions.

Let us imagine a 2-cell system as follows:

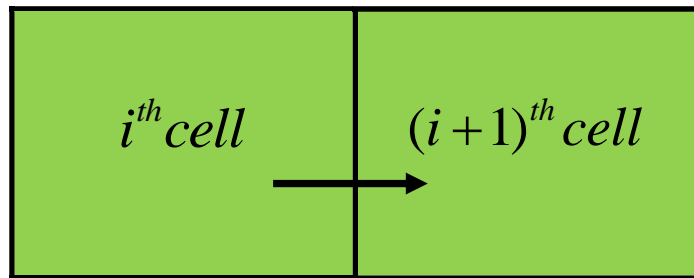


Figure 9: Two Cell Representation of Flow

Along X- and Y- directions, the fine scale transmissibilities calculated are:

$$T_{x,i} = C \frac{\left[\frac{\Delta x_{i+1} (\Delta y_i \Delta z_i) + \Delta x_i (\Delta y_{i+1} \Delta z_{i+1})}{\Delta x_i + \Delta x_{i+1}} \right]}{\left(\frac{\frac{\Delta x_i}{k_{x_i}} + \frac{\Delta x_{i+1}}{k_{x_{i+1}}}}{2} \right)} \dots\dots\dots (6)$$

And,

$$T_{y,i} = C \frac{\left[\frac{\Delta y_{i+1} (\Delta x_i \Delta z_i) + \Delta y_i (\Delta x_{i+1} \Delta z_{i+1})}{\Delta y_i + \Delta y_{i+1}} \right]}{\left(\frac{\frac{\Delta y_i}{k_{y_i}} + \frac{\Delta y_{i+1}}{k_{y_{i+1}}}}{2} \right)} \dots\dots\dots (7)$$

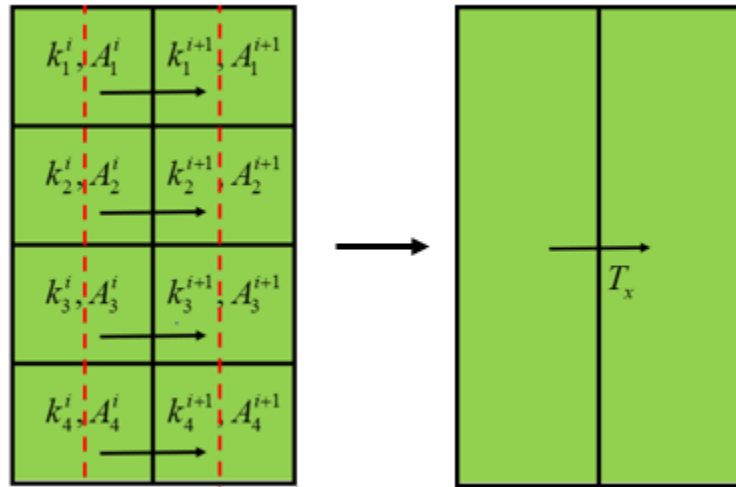


Figure 10: Transmissibility Upscaling Along Horizontal Direction

Therefore, for the upscaled transmissibilities, we have:

$$T_x = \sum_{i=1}^N T_{x,i} \dots\dots\dots (8)$$

And,

$$T_y = \sum_{i=1}^N T_{y,i} \dots\dots\dots (9)$$

Now, the calculations for the Z-direction are comparatively more complicated than X- or Y- directions. Let us imagine a system of cells as follows:

In order to understand our method of Z-direction transmissibility upscaling, we begin by calculating the Z-transmissibilities over the fine scale model (refer Figure 8), as follows:

$$T_{z,i} = C \left[\frac{\Delta z_{i+1} (\Delta x_i \Delta y_i) + \Delta z_i (\Delta x_{i+1} \Delta y_{i+1})}{\Delta z_i + \Delta z_{i+1}} \right] \dots\dots\dots (10)$$

$$\left(\frac{\Delta z_i}{k_{z_i}} + \frac{\Delta z_{i+1}}{k_{z_{i+1}}} \right)$$

$$2$$

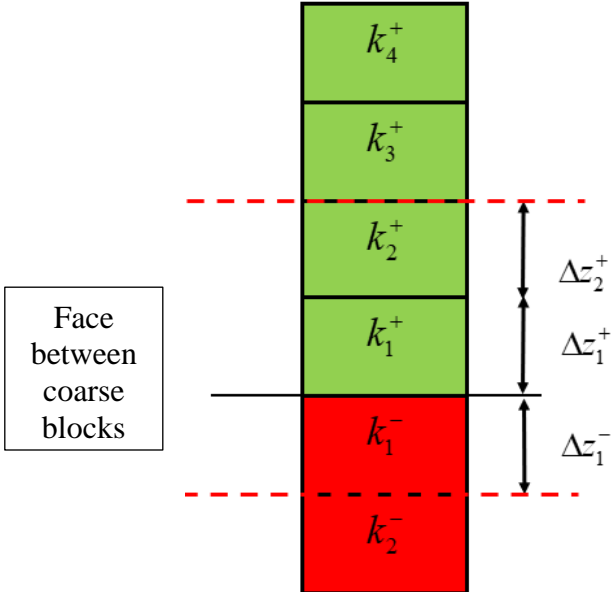


Figure 11: Transmissibility Upscaling Along Vertical Direction

However, the Δz of the fine cells are chosen such as the part of the cells within the pressure boundaries only contribute to the transmissibility calculations.

Then the coarsened transmissibility is calculated as:

$$T_z = \frac{1}{\sum_{i=1}^N \left(\frac{1}{T_{z,i}} \right)} \dots\dots\dots (11)$$

Referring to Figure 1, simulation grid design, upgridding and upscaling are the operations performed while transitioning from the static model to the simplified dynamic model. Numerical simulations on large geological models being too expensive in terms of computational time, since multiple simulations need to be run in order to optimize among various parameters. As advancement in technology continues, the geological model sizes have also been significantly increasing. Hence, upgridding and upscaling remain an important component of the reservoir modeling workflow.

A good upgridding and upscaling operation preserves the most important flow characteristics of the geologic models. However, achieving a successful upgridding and upscaling scheme has always been a major challenge, especially for high contrast geologic models. We will now discuss the reasons leading to improvement in existing upgridding techniques.

Motivation: Issues with Existing Upgridding Techniques

Following are the issues encountered with SWIFT while testing it on Amellago carbonate model:

- **Apparent Preservation of Heterogeneity:** Variance-based upgridding shows an apparent preservation of heterogeneity to almost 100% even at very few layers. This inherently neglects the contribution to the heterogeneity by most layers, such that even

when the model has been coarsened to fewer than one-tenth the original number of layers (Velocity and Slowness plots from Figure 12), normalized variance preserved is very close as the fine-scale model (preservation of at least 90% variance at about 100 layers).

For the VxS plot (in green), the layer merging is based on Eqn.(27) and the plotting of the heterogeneity curve is according to Eqn. (29)

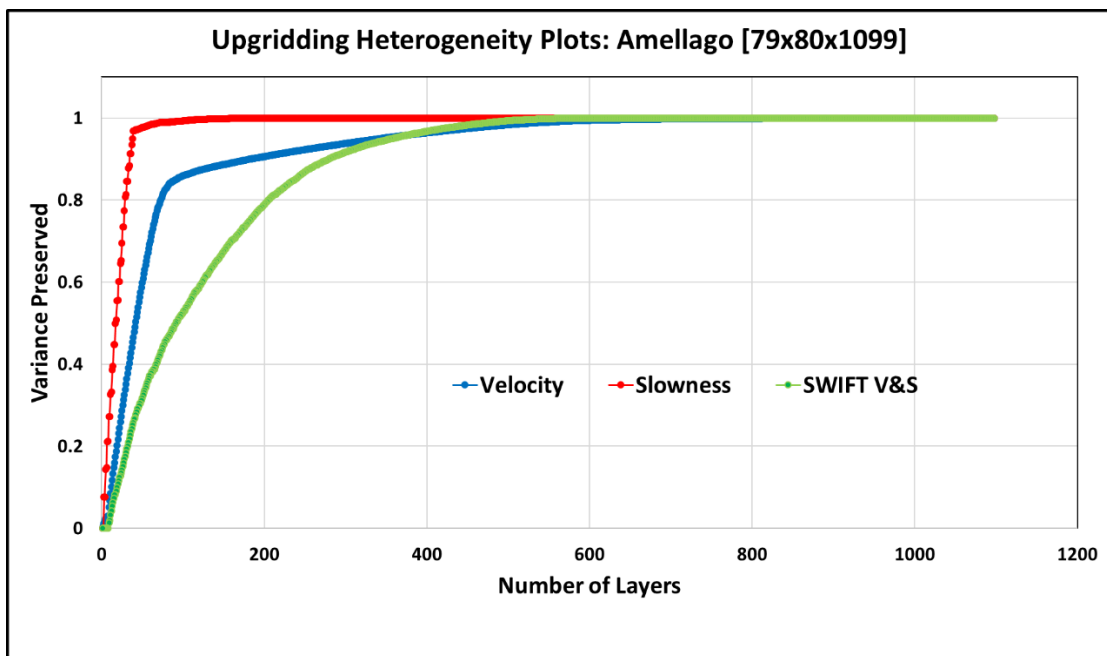


Figure 12: Upgridding Heterogeneity Plots for Amellago Carbonate Model

- **Collapse of fine scale layers:** Associated with the apparent preservation of heterogeneity, we find that very many fine layers are grouped into a single or very few coarse layers. Often the entire zone collapses into a single coarsened layer. This phenomenon is a manifestation of the apparent preservation of heterogeneity, discussed previously. Results of the optimal layer design are shown in Figure 13.

Following Figure 12, we observe how the zones of Amellago carbonate model have been coarsened. Some zones, especially low permeability zones like ISO-hg4 and ISO-s3 (the ones highlighted in yellow) have been very aggressively coarsened by factors of 46.3 and 68 respectively. Also, we notice how the coarsened number of layers for any particular zone vary with the choice of variance calculation. For ISO-hg4 (2nd zone), Velocity assigns very aggressive coarsening while Slowness coarsens the model moderately with coarsening ratio of 9.3. We see the same trend in other low permeability zones. Higher permeability zones show preservation of a greater number of layers by Velocity variance calculation method.

Zones	PermX	Average Porosity	Fine Layers	Number of Fine Layers	Vn-Column Avg			Ratios		
					Velocity	Slowness	VxS			
ISO-s4	139.27	0.06	1 - 158	158	50	7	4	3.2	22.6	39.5
ISO-hg4	19.52	0.05	159 - 343	185	4	20	21	46.3	9.3	8.8
ISO-hg3	380.71	0.13	344 - 408	65	42	14	28	1.5	4.6	2.3
ISO-hg1	114.72	0.04	409 - 620	212	36	31	35	5.9	6.8	6.1
ISO-s3	52.12	0.12	621 - 688	68	1	23	2	68.0	3.0	34.0
ISO-s2	127.46	0.16	689 - 741	53	3	20	1	17.7	2.7	53.0
ISO-s1	198.68	0.13	742 - 804	63	16	7	2	3.9	9.0	31.5
ISO-base	99.07	0.03	805 - 1099	295	32	62	91	9.2	4.8	3.2
Total	115.16	0.06	1 - 1099	1099	184	184	184			
Optimal Number of Layers					99	80	316			

Figure 13: Layering Summary for SWIFT Coarsening for Amellago Carbonate Model

- **Choice of Weighting Factors:** For clastic reservoirs we define NTG to differentiate sand from non-sand zones. However, for high contrast carbonate reservoirs NTG may not be defined. Previously, we have used the net rock volume as the pre-factor in all the variance calculations. However, net rock volume tends to overestimate the contribution of heterogeneity especially from low permeability regions with high

values of slowness which reduces to the bulk rock volume in models without an explicit net/non net cutoff. An example is the Amellago model. This can be seen in Figure 14. While considering the weights as rock volume, the volume is almost uniformly distributed over the areal map, however, when we look at the column average porosity and permeability maps, we notice that most of the zone is very low quality with very few good quality patches of high porosity and high permeability. Introducing a weight that is more characteristic of the reservoir quality is expected to provide a more useful error measure.

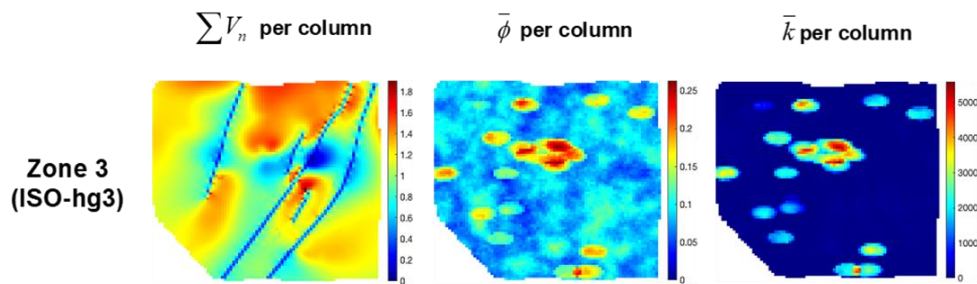


Figure 14: 2D Areal Map of Zonal Net Rock Volume, Average Porosity and Average Permeability

Owing to these problems encountered, we started probing deeper into the physics of our variance calculations, error measures and upgridding algorithms.

We started off by testing how our existing algorithms work when cutoffs are introduced into the model. Following the cutoffs, we tested variations of weighting factors in calculation of error measures for grouping layers. While these seemed to be only peripheral modifications to the mathematics of the calculations, we also formulated

different averaging techniques for preservation of the characteristic of every zone. These have been named as ‘Zonal Averaging’ and ‘Zonal Upgridding’.

Finally, these paved way for developing the novel distance based upgridding technique, which will be dealt with in details in chapter 4 of the dissertation.

CHAPTER II

LITERATURE REVIEW

Coarsening of high-resolution 3D geologic models by layer grouping and assigning effective properties for the coarsened grid have been studied since the 1990's and it remains a useful part of the reservoir modelling workflow. In this chapter of the dissertation, we will review the physical and mathematical background of our understanding of layer grouping which will provide the foundation to extend our understanding of how to improve the layer coarsening or upgridding of geologic models. I have categorized this section into 3 major segments as depicted in the figure below.

The first column in Figure 15 includes the very early works of establishing how static properties of cells would help in grouping layers. The second column is theoretically the starting point of my research where we establish a very accurate measure of heterogeneity that could be used to group layers. Finally, the third column mentions the upgridding software SWIFT (Petrel plug-in) and the results of which were used as the base cases for all the research developments.

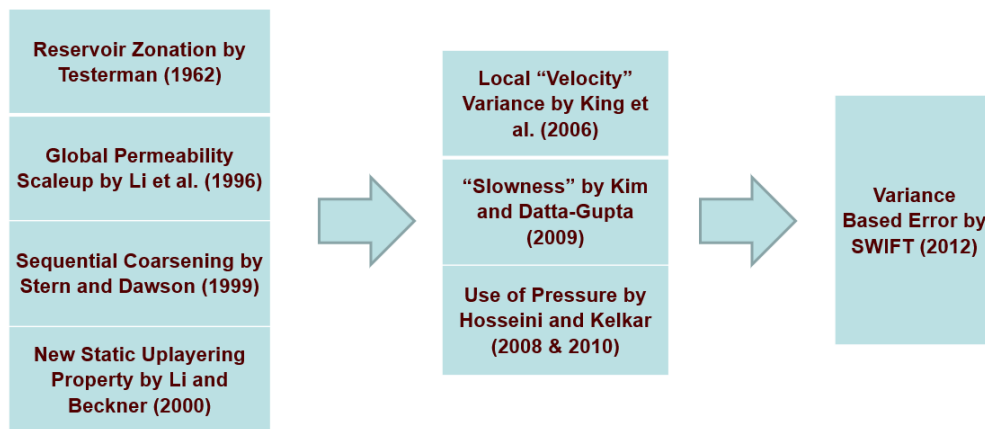


Figure 15: Chronology of Technical Advancements in Upgridding

Testerman (1962)

Layer coarsening is closely related to the specification of a statistical variance-based reservoir-zonation technique studied by Testerman (1962). According to Testerman (1962), it was a statistical technique to correlate naturally occurring zones in a reservoir from well to well. It started off as an aid to predicting or interpreting fluid displacements during recovery processes with an aim to organize the large amount of core analysis data. Thus, the need for grouping of permeability data. One may ask how this theoretical development relates to upgridding. The answer to that is “Reservoir Zonation” technique proposed here.

First, the set of permeability data at a single well is divided into zones. Most common method used was to group the permeability data based on ranking according to capacity-fraction technique. This ranks permeabilities in order of magnitude, regardless of the physical location of the permeabilities within the reservoir. This has led to grouping of layers in 3D geologic models based on ranking of permeabilities, as a tool for layer coarsening in the subsequent research

Zonation aimed at capturing which zones are likely to be continuous between wells. This led to one of the early ideas of grouping multiple layers of a geologic model into a coarsened layer, thereby decreasing the resolution while preserving the characteristics of the higher resolution model. The zonation of individual wells was performed by minimizing the variation of permeability within the zones and maximizing the variation between the zones. Mathematically,

$$B = \frac{1}{L-1} \left[\sum_{i=1}^L m_i (\bar{k}_i - \bar{k}_{well})^2 \right] \dots\dots\dots (12)$$

$$W = \frac{1}{N-L} \left[\sum_{i=1}^L \sum_{j=1}^{m_i} (k_{ij} - \bar{k}_i)^2 \right] \dots\dots\dots (13)$$

$$R = \frac{B-W}{B} \dots\dots\dots (14)$$

where B = the variance between zones, L = the number of zones, i = the zone index, j = the data point index within the zone, m_i = the number of data points in the i th zone, \bar{k}_i = the mean of the permeability data in the i th zone, \bar{k}_{well} = the over-all mean of the data in the well, W = the pooled variance within zones, N = the total number of data points, k_{ij} = the j th permeability data point in the i th zone, and R = the zonation index.

Thus, “Between (B)” and “Within (W)” parameters for variance-based error measures were calculated. The permeability data was divided in their original order of depth, into all possible combinations of two zones. ‘ B ’, ‘ W ’ and ‘ R ’ were calculated for each of those possible two-zone combinations, according to Eqns. (12), (13) and (14) respectively. The zonation index (R) is the criterion to denote the best division. This index varies from 0 to 1.0 and indicates how closely the division corresponds to homogenous zones. The closer the index is to 1.0, the more homogeneous the zones. Hence, larger the index denotes best division into two zones and is stored in memory to compare with other indices. After successfully combining the best two-zone, the data is divided into all possible three-zone combinations. Subsequently, the data gets divided into four-zone combinations and so on, until two successive indices show no significant difference.

After individual wells were zoned, multiple adjacent wells were correlated throughout the reservoir to be able to determine the continuity of the strata.

This technique was proposed to be general and could be extended to quantify reservoir heterogeneity by using reservoir properties other than permeability. Also, the zonation schemes developed based on the analysis of individual wells were subsequently extended to multi-well data. Later, the idea of grouping layers based on permeabilities, minimizing the variance within each layer and maximizing the variance between layers, led to the development of statistical upgridding by later researchers.

Durlofsky et al. (1996)

Durlofsky et al. (1996) attempted at scaling up of highly detailed, heterogeneous, 3D geological models. This method involves non-uniform coarsening followed by appropriate assignment of properties to the coarsened model. Here, we will focus on the grid coarsening aspect of this paper. The determination of the structure of the coarsened grid requires efficient identification of high flow regions in the model. Solving for pressure across the entire fine scale model helps to determine the dominant flow regions and leads to selectively group layers.

They implemented two techniques:

- “Composite Solve”: Computationally efficient but less accurate method of solving a sequence of cross-sectional, single phase flow problems with flow driven by generic pressure boundary conditions

- Rigorous and computationally expensive, however more accurate method of solving single phase flow problem for actual injection and production wells.

These methods help determine regions of potentially high flow. Average flow rate through each layer is used to determine the new grid. The basic structure of the coarse grid is based on the number of fine scale grid blocks in the x -, y - and z - directions to be coarsened into a single coarse block. The volumetric flow rate through each coarse layer can be approximated as the sum of the flows through all the fine scale layers comprising that particular coarsened block. Then, if the total flow rate through the coarsened layers exceed a prescribed fine scale flow rate, then coarsened layers are subdivided into finer layers. This process continues until the specification on total flow rate through any coarse layer is satisfied. As a result, this method introduces refinement into the high flow regions of the model.

Li et al. (1996)

Following the findings of Testerman (1962), Li et al. (1996) introduced a global permeability scaleup method designed to maximally preserve the variance and spatial correlation of an entire 3D permeability field. This included scaling up of the absolute permeability field by flux-averaging, averaging fine grid relative permeabilities and capillary pressures. It also included the formulation of pseudo-functions by superposition of the fractional flow curves.

Stern and Dawson (1999)

Stern and Dawson (1999) developed a sequential coarsening algorithm, where they combined layers sequentially to minimize the changes in geological model properties. They developed objective functions in terms of the change in the time required for single-phase early water breakthrough in both fine and coarse grids and in terms of differences of flux between fine and coarse grids, for selecting optimal locations for simulation model layer boundaries and also determining the number of layers required.

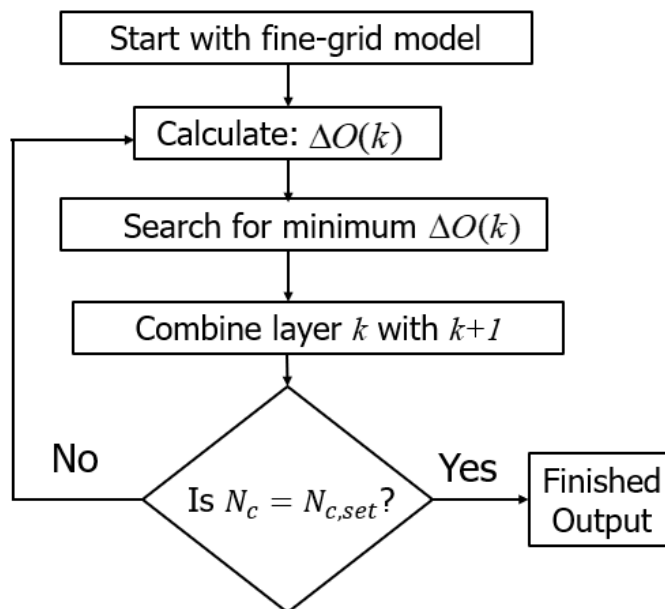


Figure 16: Procedure for Layer Selection (Stern and Dawson (1999))

Li and Beckner (2000)

Li and Beckner (2000) proposed a new static uplayering (upgridding) property, which was not just the cell permeability. This property was a combination of porosity, permeability

and facies (in terms of relative permeability, endpoint saturation and various facies rules). Diagnostic measures of this method included generation of a residual curve.

Fincham et al. (2004)

Fincham et al. (2004) also made a study of upgridding from geological models to simulation models. This involved construction of coarse grids, both uniform and non-uniform coarsening. They followed two methods already developed by prior researchers: Stern and Dawson (1999) and (Durlafsky, 1996)

King et al. (2006)

We will now describe the approach of King et al. (2006) as it provides the starting point of the current research. It describes the local velocity of a waterflood flood front. King et al. (2006) developed a new optimized upgridding algorithm for coarsening 3D geologic models, utilizing local velocity variance as an error measure to quantify the static measure of heterogeneity. This method is different from the previous methods mentioned by using a more accurate measure of heterogeneity and by being based on recursive sequential coarsening. The local velocity is the product of the Buckley-Leverett velocity and interstitial flow velocity within each cell of the fine grid. The local velocity can be directly related to the fluid flow in the porous media.

Velocity is mathematically defined as:

$$Velocity, V = f \cdot \frac{k}{\phi} \dots\dots\dots (15)$$

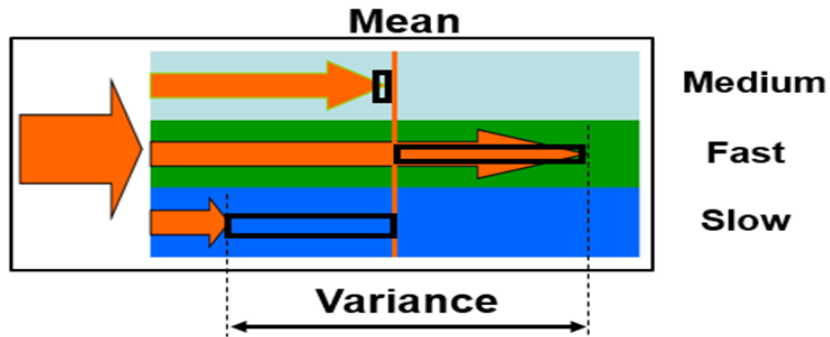


Figure 17: Frontal Velocity Variance used as Error Measure

Figure 17 illustrates how the frontal velocity variance is used as an error measure between subsequent layers in a multi-layered model. In the figure, the length of the orange solid arrows represents the magnitudes of the velocity fronts. The black boxes represent the corresponding variances calculated about the vertical orange line, which is the mean velocity for those layers.

Kim and Datta-Gupta (2009)

Kim and Datta-Gupta (2009) attempted to preserve the spatial variations of streamline time of flight representing water saturation front propagations while grouping layers. Hence, their choice of static property to measure error was different from King et al. (2005). They preserved the “Slowness” distribution between the fine and coarse-scale models.

Slowness is mathematically defined as:

$$Slowness, S = \frac{\phi}{k} \dots\dots\dots (16)$$

While the velocity variance was more sensitive to fluid breakthrough, minimization of the slowness variance better preserved barriers.

Hosseini and Kelkar (2008) and (2010)

Hosseini and Kelkar (2008) introduced the use of pressure or $\left(\frac{1}{k}\right)$ in calculating the error, instead of velocity (King et al. 2006). Starting with their theory of 2008, Hosseini and Kelkar (2010), recognized that their approach minimized the variance in both velocity and slowness.

Mathematically for a system of two adjacent grid blocks with indexes of (i, j, k_1) and (i, j, k_2) , and h_{ijk} as the corresponding cell heights, the error based heterogeneity term can be represented as:

$$E_T = \sum_{ij} \sqrt{\left[\frac{k_{ijk_1}^2 h_{ijk_1}^2 + k_{ijk_2}^2 h_{ijk_2}^2}{(k_{ijk_1} h_{ijk_1} + k_{ijk_2} h_{ijk_2})^2} \right] \left[\frac{(k_{ijk_1} - k_{ijk_2})^4}{(k_{ijk_1} k_{ijk_2})^2} \right]} \dots\dots\dots (17)$$

This error is calculated from a combination of the differences in permeability and the inverse of permeability for cells in adjacent layers.

SWIFT (2012)

Versions of these concepts have been implemented in SWIFT: an upgridding research application developed by our research group. The following set of equations give a brief outline of the algorithms implemented in SWIFT.

Following King et al. (2006) and Kim and Datta-Gupta (2009), we begin by calculating the total heterogeneity as:

$$H = \sum_{i,j,k=1}^{NX,NY,NZ} n_{ijk} (P_{ijk} - \bar{P}_{ij})^2 \dots\dots\dots (18)$$

Here, n_{ijk} = Net Rock Volume and, P_{ijk} = Velocity (V_{ijk}) or Slowness (S_{ijk})

The averaged property was calculated for each column of the model as:

$$\bar{P}_{ij} = \frac{\sum_{k=1}^{NZ} n_{ijk} P_{ijk}}{\sum_{k=1}^{NZ} n_{ijk}} \dots\dots\dots (19)$$

This column average is used as the reference for the variance calculation. When we merge two adjacent layers k_1 and k_2 , the property P_{ijk} is coarsened.

$$P_{ijk}^C = \frac{n_{ijk_1} P_{ijk_1} + n_{ijk_2} P_{ijk_2}}{n_{ijk_1} + n_{ijk_2}} \dots\dots\dots (20)$$

Also,

$$n_{ijk_1}^C = n_{ijk_1} + n_{ijk_2} \text{ and } n_{ijk_2}^C = 0 \dots\dots\dots (21)$$

Now, we quantify the heterogeneity remaining in the model. Following the usage of Testerman (1962), this is the ‘‘Between’’ cell heterogeneity.

$$B = H(P^C) = \sum_{i,j,k=1}^{NX,NY,NZ} n_{ijk} (P_{ijk}^C - \bar{P}_{ij})^2 \dots\dots\dots (22)$$

When we merge the two layers k_1 and k_2 , the ‘‘Between’’ cell heterogeneity will always decrease.

$$\delta B = - \sum_{i,j}^{NX,NY} \frac{n_{ijk_1} n_{ijk_2}}{n_{ijk_1} + n_{ijk_2}} (P_{ijk_1}^C - P_{ijk_2}^C)^2 \dots\dots\dots (23)$$

This property is known to be monotonic and guarantees that the coarsened reservoir models are less heterogeneous than fine.

We define “Within” cell heterogeneity as follows:

$$W = H - B \dots\dots\dots (24)$$

This “Within” cell heterogeneity expression looks like:

$$W = \sum_{i,j,k=1}^{NX,NY,NZ} n_{ijk} (P_{ijk} - P_{ijk}^C)^2 \dots\dots\dots (25)$$

Given Eq.(24) , the total heterogeneity for a particular model is always constant, irrespective of the degree of coarsening. For this method, we obtain:

$$\delta W = -\delta B \dots\dots\dots (26)$$

Minimization of δW is used to decide upon the sequence of layers to merge in going from the fine scale to the coarser models.

For the combined error measure based on both Velocity and Slowness, SWIFT uses the following definitions for the minimization property used to decide upon the sequential coarsening and for the calculation of the “Between Cell” heterogeneity.

$$\delta W_{VS} = \sum_{i,j}^{NX,NY} \sum_{k=k_1,k_2} n_{ijk} \left| \left(V_{ijk} - \frac{\bar{k}_{ij}}{\bar{\phi}_{ij}} \right) \left(S_{ijk} - \frac{\bar{\phi}_{ij}}{\bar{k}_{ij}} \right) \right| \dots\dots\dots (27)$$

Here, $\bar{\phi}_{ij}$ and \bar{k}_{ij} are the net rock volume weighted averages of the porosity and the permeability in each column. We use δW to sequentially merge layers based on identifying the pair of adjacent layers corresponding to the minimum value of δW . After coarsening, the heterogeneity is computed following Eq.(28).

The entire workflow for SWIFT can be summarized as follows:

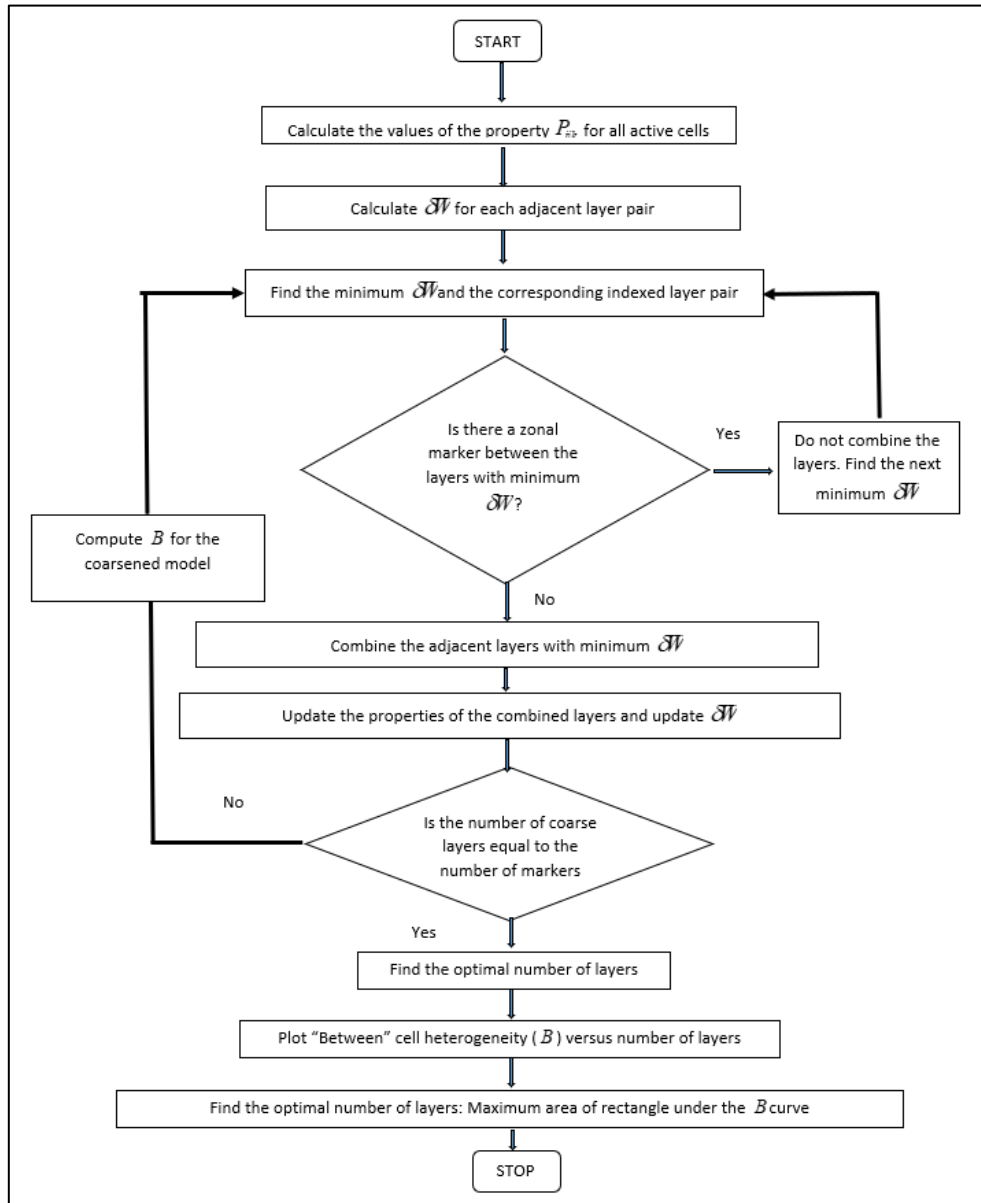


Figure 18: Workflow of SWIFT

Calculation of the heterogeneity preserved in the coarsened model is based on B_{VS} according to Eqn.(28).

$$B_{VS} = \sum_{i,j,k=1}^{NX,NY,NZ} n_{ijk} \left| \left(V_{ijk}^C - \frac{\bar{k}_{ij}}{\bar{\phi}_{ij}} \right) \left(S_{ijk}^C - \frac{\bar{\phi}_{ij}}{\bar{k}_{ij}} \right) \right| \dots\dots\dots (28)$$

Crossover curves plotting heterogeneity preserved in the model as the number of layers are reduced are drawn. We begin by plotting the heterogeneity contained in the fine scale model, i.e. 85 layers for SPE10. As we reduce the number of layers, the heterogeneity preserved in the coarsened model sequentially decreases, until we reach a single layer model which is totally homogeneous. Each point on the curve is plotted by optimizing the heterogeneity preserved for that particular number of layers.

Figure 19 is an Upgridding heterogeneity plot for SPE10, which is a reference model used in the upscaling literature. These curves depict the degree of loss of heterogeneity as a model is sequentially coarsened.

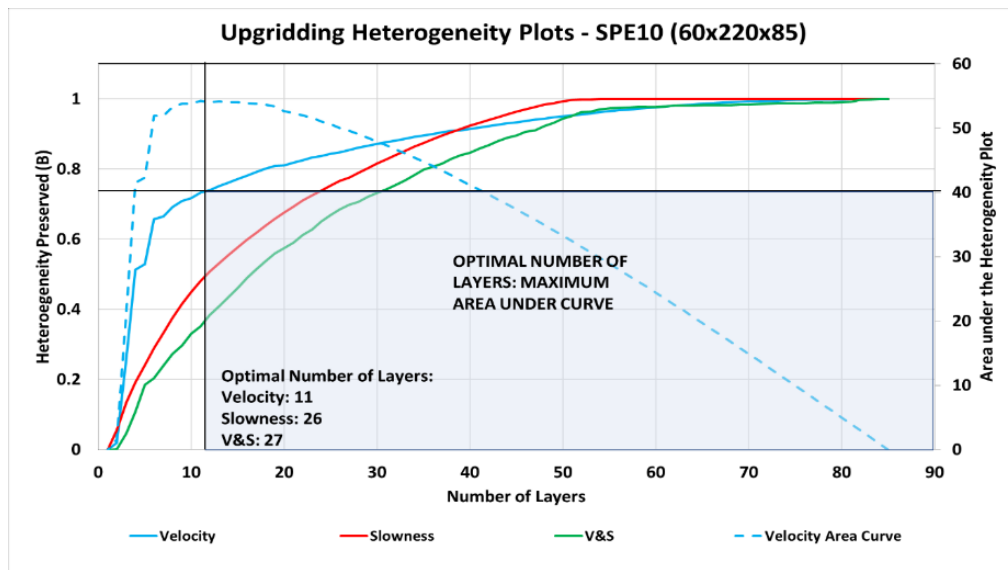


Figure 19: Upgridding Heterogeneity Plots for SPE10 Model along with the method of selection of Optimal Number of Layers: Maximum Area Method

These curves are also used to identify the optimal number of layers.

This curve is drawn for the corresponding number of layers in the coarsened model by plotting the following equation:

$$\textit{Heterogeneity Preserved}, HP_k = 1 - \left(\frac{B_{\min} - B_k}{B_{\min}} \right) \dots\dots\dots (29)$$

Optimal layer designs are based on a maximum quality calculation (per geologic unit). The optimal number of layers is calculated by maximizing the cost efficiency (reduction in the number of layers) and fidelity (calculated variance) simultaneously. In order to achieve that, a heterogeneity plot of B versus the number of layers is used and a “break point” is chosen along the curve beyond which the heterogeneity reduces severely as the number of layers decreases. Referring to Figure 19, the “break point” is chosen at which the rectangular area under the heterogeneity curve is maximized.

CHAPTER III

IMPROVED UPGRIDDING TECHNIQUES

Despite the utility of the existing algorithms, there were a number of short-comings. While our existing upgridding algorithms offered satisfactory results with SPE10 (a sandstone model), we faced anomalous and less practical outcomes with models with greater variations in spatial distribution of heterogeneity. As a test case, we used Amellago carbonate outcrop model. In this chapter, I would discuss some of the preliminary statistical alterations that I performed based on our prior art Variance based error analysis to understand how the heterogeneity is being quantified and therefore use it as a proper representation to coarsen models.

Improved Upgridding: Introduction of Cutoffs

In the Literature Review section, we have already discussed how the heterogeneity plots (crossover curves) look like and what inference can be drawn from them. Here, in this section we will go through those curves in details, along with some of the layering schemes for different cases on the Amellago model, introducing different cutoffs.

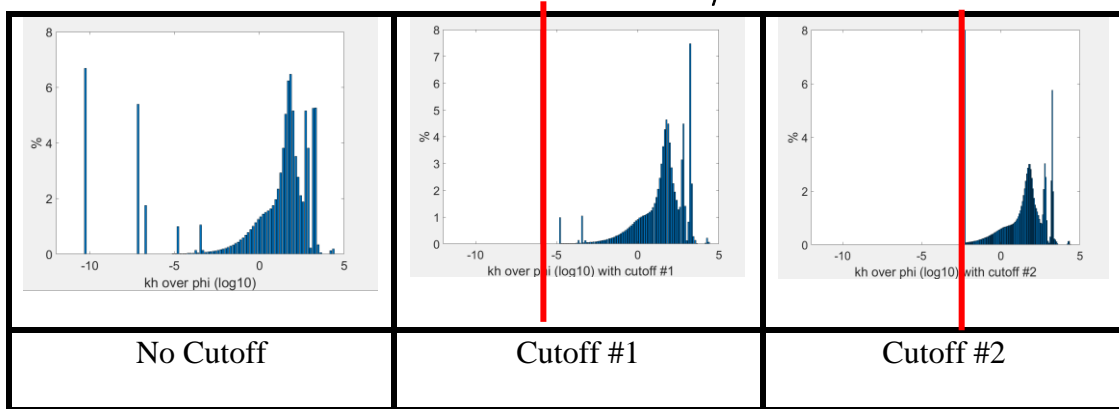
To begin with, in most of the conventional clastic geologic models, a sense of net/non-net pay is embedded into the model itself. Hence, parts of the model which are negligible towards contribution to flow are discarded inherently. However, for the carbonate model at hand, there has been no net/non-net in the model. To improvise one such factor into the model we would need the help of property distributions, as depicted in the Figure 4.

Among those histograms, we choose to use the $\frac{k_H}{\phi}$ plots for deciding where the non-net would be defined.

The cutoffs are defined as follows:

- Cutoff #1: If $\frac{k_H}{\phi} < 1 \times 10^{-6}$, then NTG = 0
- Cutoff #2: If $\frac{k_H}{\phi} < 0.005$, then NTG = 0

Table 5 - Choice of cutoff based on $\frac{k_H}{\phi}$ Distributions



Following are the results of Layer grouping when applied to the existing SWIFT upgridding calculations. Table 6 depicts the effect of cutoffs on the layering scheme of the coarsened models of Amellago for all the error measures. The x-axis of the column chart is the “Coarse Layer Number” and the y-axis is “Number of Fine Layers” in those coarsened layers. In all the cases, optimal coarsening was applied, and a simulation constraint of a maximum of 12 fine layers to be merged into any single coarsened layer was followed. It is observed that certain sections of the model retain the fine-scale resolution even after coarsening (e.g. Velocity). However, for certain error measures such

as Slowness we notice a significant impact of cutoffs. This is due to the removal of the low permeability cells when the cutoffs were enforced on the model.

Table 6 - SWIFT Layering Distribution for Amellago Carbonate Model

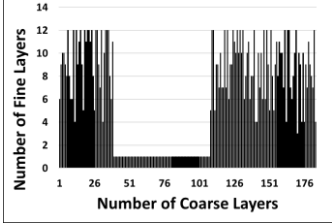
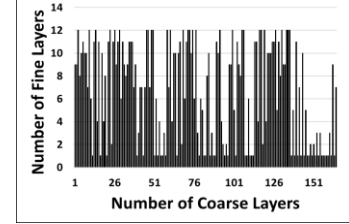
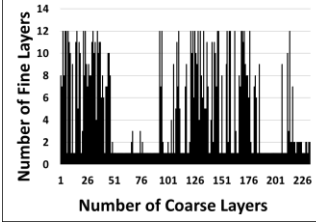
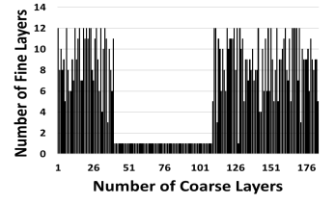
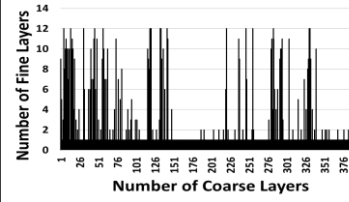
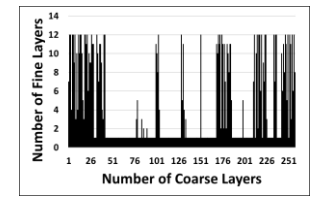
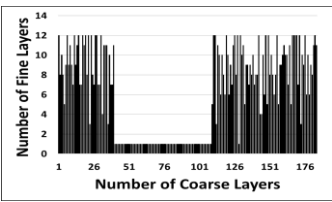
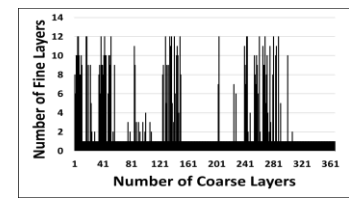
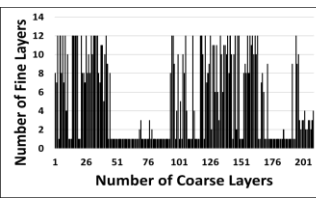
Velocity	Slowness	V&S
		
No Cutoff	No Cutoff	No Cutoff
		
Cutoff #1	Cutoff #1	Cutoff #1
		
Cutoff #2	Cutoff #2	Cutoff #2

Table 7 - Comparison of Cutoffs in Distribution of Fine Layers into Coarse Layers

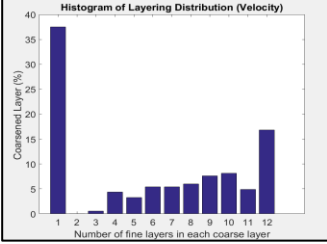
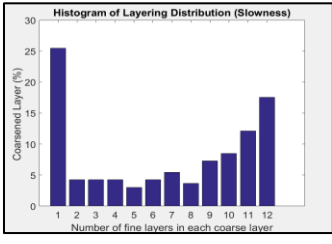
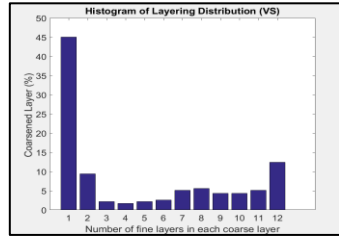
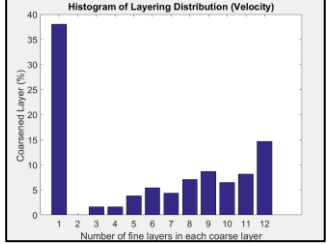
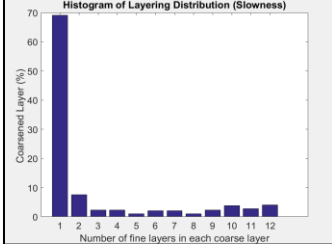
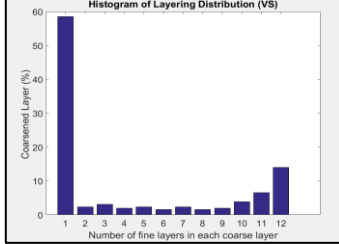
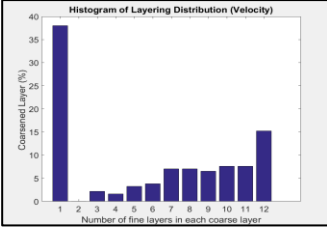
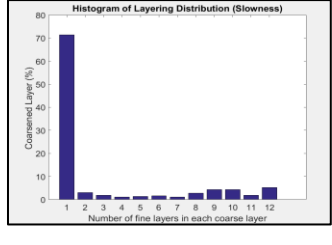
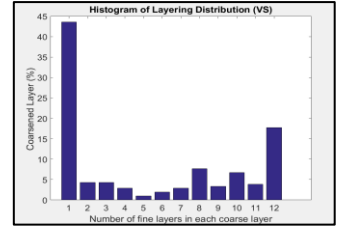
Velocity	Slowness	V&S
 <p>Histogram of Layering Distribution (Velocity)</p> <p>Coarsened Layer (%)</p> <p>Number of fine layers in each coarse layer</p>	 <p>Histogram of Layering Distribution (Slowness)</p> <p>Coarsened Layer (%)</p> <p>Number of fine layers in each coarse layer</p>	 <p>Histogram of Layering Distribution (VS)</p> <p>Coarsened Layer (%)</p> <p>Number of fine layers in each coarse layer</p>
No Cutoff	No Cutoff	No Cutoff
 <p>Histogram of Layering Distribution (Velocity)</p> <p>Coarsened Layer (%)</p> <p>Number of fine layers in each coarse layer</p>	 <p>Histogram of Layering Distribution (Slowness)</p> <p>Coarsened Layer (%)</p> <p>Number of fine layers in each coarse layer</p>	 <p>Histogram of Layering Distribution (VS)</p> <p>Coarsened Layer (%)</p> <p>Number of fine layers in each coarse layer</p>
Cutoff #1	Cutoff #1	Cutoff #1
 <p>Histogram of Layering Distribution (Velocity)</p> <p>Coarsened Layer (%)</p> <p>Number of fine layers in each coarse layer</p>	 <p>Histogram of Layering Distribution (Slowness)</p> <p>Coarsened Layer (%)</p> <p>Number of fine layers in each coarse layer</p>	 <p>Histogram of Layering Distribution (VS)</p> <p>Coarsened Layer (%)</p> <p>Number of fine layers in each coarse layer</p>
Cutoff #2	Cutoff #2	Cutoff #2

Table 7 is a histogram listing the frequency of coarsened layers corresponding to the number of fine layers they contain. This is a similar depiction of what we observed in Table 6. Here, we observe two major peaks:

- Preservation of fine scale resolution: A large number of coarsened layers have only a single fine layer. In other words, the resolution of the fine scale model is preserved in those coarsened layers.
- Simulation constraint: As a simulation constraint had been imposed on the coarsening schemes, we observe a large number of coarse layers to have maximum allowable fine layers in them. When the constraint was lifted, it was observed to have more than 12 layers being combined into a single coarsened layer.

As an inferential comment, we can tell that introduction of cutoffs necessarily does not fix the problem. However, it is easier to formulate our understanding of net/non-net in high contrast geologic (carbonate) models.

Table 8 - Effect of Cutoffs on the Optimal Number of Layers (Amellago)

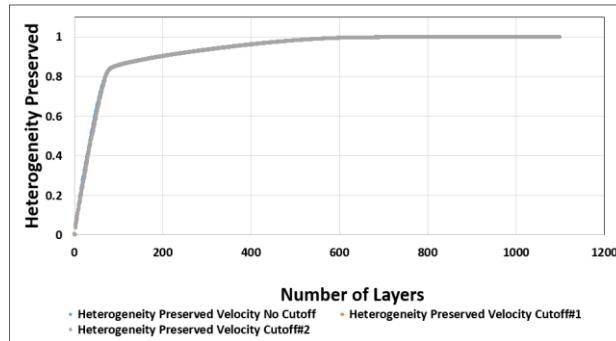
Algorithms (Error Measures)	Optimal Layer Count		
	No Cutoff	Cutoff#1	Cutoff#2
Velocity	184	184	184
Slowness	165	399	367
V&S	233	258	209

Table 8 shows the effect of cutoffs on the optimal number of layers for Amellago. Considering ‘Velocity’ error measure, introduction of cutoffs does not quite exhibit much change in the layering distributions and optimal number of layers. This can be further explained by the fact that introducing cutoffs only removes the very low permeability cells which negligibly contribute to the magnitude of velocity calculations. Hence, the similar layering schemes irrespective of cutoffs. However, for ‘Slowness’ error measure, neglecting the low permeability cells actually restricts the maxima of Slowness and makes it more sensitive to the permeability distribution of the model. We see a greater number of layers in the optimal coarsened model, when using ‘Slowness’ error measure. ‘V&S’ exhibits characteristic mid-way between ‘Velocity’ and ‘Slowness’.

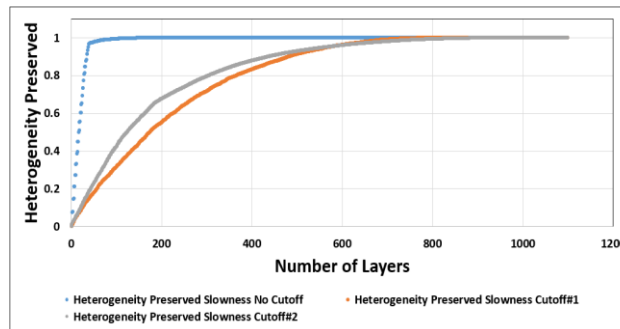
In Figure 20 below we have a comparison of the effects of cutoffs on the heterogeneity plots for the layering schemes from various error measures. As shown before, Velocity remains almost unaltered, while Slowness heterogeneity plots show signs of improvement when using cutoffs. We do not want a great amount of heterogeneity (~100%) to be preserved even at very low layer counts. Cutoffs make sure the heterogeneity plots do not get too aggressive while coarsening optimally.

‘V&S’ heterogeneity plots exhibit a jagged or rather sudden breaks/jumps along the coarsening scheme as we reduce the number of layers. In the later section of our discussion, we have attempted successfully to remove the breaks/jumps and made the combination of ‘Velocity’ and ‘Slowness’ more continuous.

Velocity



Slowness



V&S

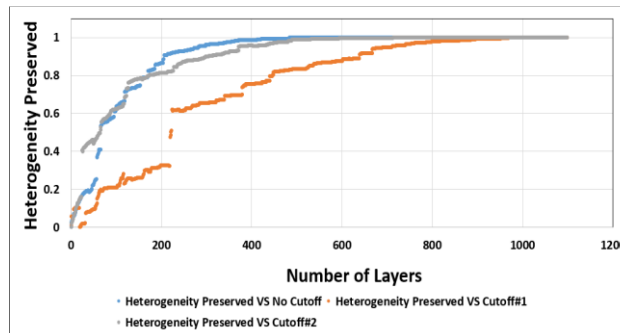


Figure 20: Upgridding Heterogeneity Plots – Comparing effects of Cutoff for various error measures

Improved Upgridding: Choice of Weighting Factors

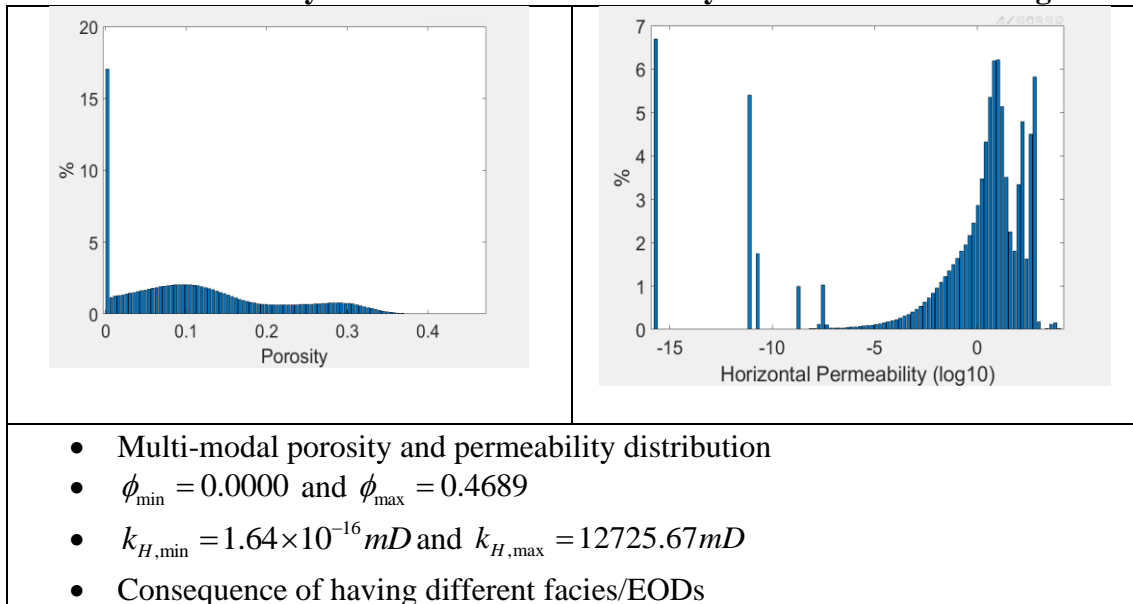
We have already noticed the effect of setting a net or non-net cutoff for cells which supposedly are not contributing to the flow capacity or storage capacity of the reservoir.

While looking through the layering schemes in each case, we noticed how the exclusion of low permeability cells do not affect the layer grouping based on ‘Velocity’ error

measure. However, on the contrary, for ‘Slowness’, the distributions with cutoffs preserved a higher degree of fine scale resolution. Since Amellago has such a wide range of property distribution (see Table 9), we probed into something more fundamental to the construction of the model, i.e. the ‘Stratigraphic Units’ or ‘Geologic Zones’. Since zonal characteristic adheres closely to the control of flow throughout the reservoir, we attempt to make sure the weighting factors going into the calculations are correct or rather more accurate.

In the existing SWIFT algorithm, we have been using Net Rock Volume (NRV). However, the storage capacity of the reservoir involves porosity and hence Pore Volume (PV) weighted calculations can be considered more accurate in capturing the spatial distribution of heterogeneity. This will be discussed and verified in this section.

Table 9 - Porosity and Horizontal Permeability Distribution of Amellago



Previously we chose the cutoffs to be defined as:

- Cutoff #1: If $\frac{k_H}{\phi} < 1 \times 10^{-6}$, then NTG = 0
- Cutoff #2: If $\frac{k_H}{\phi} < 0.005$, then NTG = 0

We choose a middle ground between the two previously chosen cutoffs, in order to preserve some of the low permeability characteristic while neglecting the very poor-quality parts of the reservoir.

As shown in Figure 21, we choose the cutoff to be: If $\frac{k_H}{\phi} < 5 \times 10^{-6}$, then NTG = 0

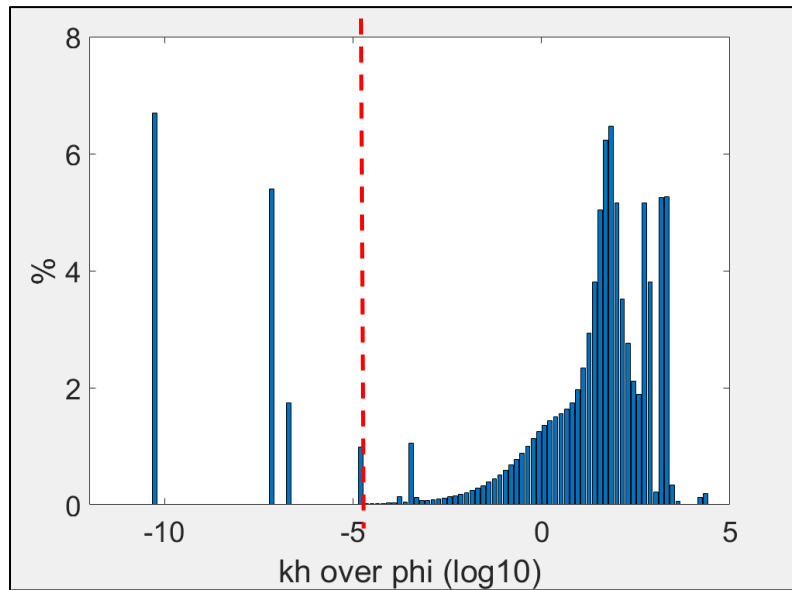
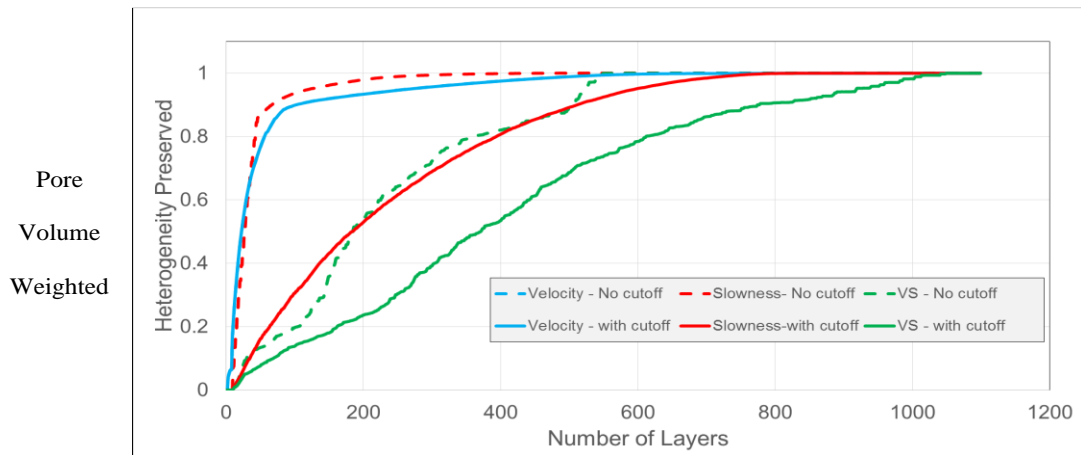
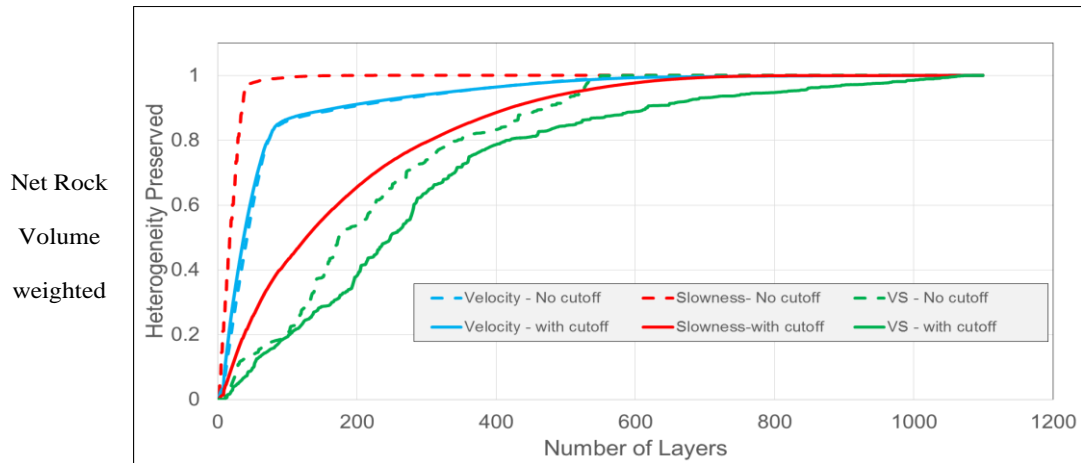


Figure 21: Choice of Cutoff to be used for Comparison of Weighting Factors



In

Figure 22, we have a comparative study of the heterogeneity plots using net rock volume or pore volume as the weighting factors. Using ‘Pore Volume’ weighted calculations, the heterogeneity plots are less aggressive and exhibits a more pragmatic loss of heterogeneity as we reduce the number of layers left in the model. However, only heterogeneity plots are not enough to decide the utility of an upgridding algorithm. In the next figure we look at the coarsened layering distributions.

Pore Volume weights clearly provides an improvement in reducing the collapse of several fine layers into a single or very few coarsened layers.

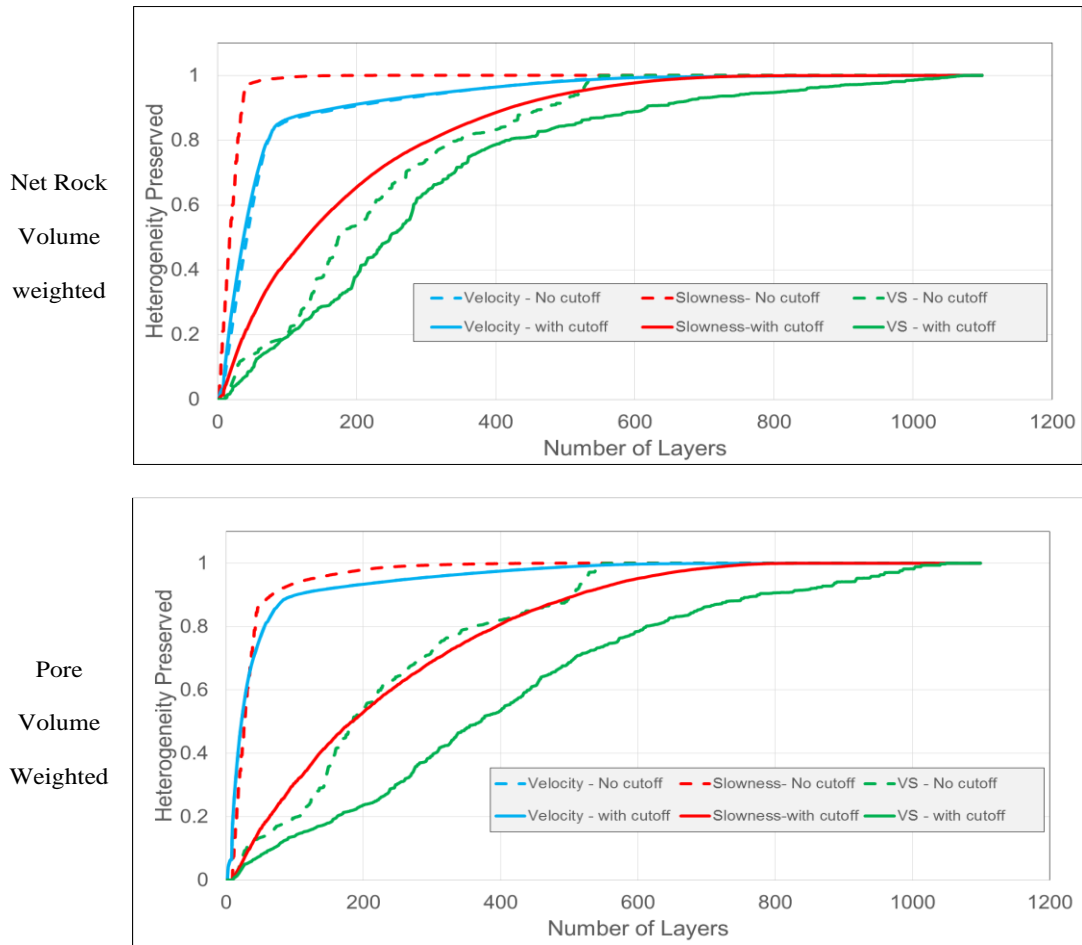


Figure 22: Upgridding Heterogeneity Plots: Comparison of Weighting Factors

Below are the layering distributions of Amellago when coarsened with net rock volume weights and pore volume weights. From Figure 23, we observe that there is no significant change in the number of coarse layers per zone and similarly no significant change in the total number of layers in the coarsened model with no cutoff. Figure 24 shows the effect of weighting factor when cutoffs are enforced and we observe the same trend of no significant change in layers per zone and in total number of layers except in a very few cases (marked by red boxes).

Zones	Layers	PermX (mD)	Average Porosity	Number of fine layers	Number of Coarse Layers					
					Net Rock Volume Weighted			Pore Volume Weighted		
					No Cutoff			No Cutoff		
					Velocity	Slowness	VS	Velocity	Slowness	VS
ISO-s4	1 - 158	139.27	0.06	158	6	5	25	3	6	28
ISO-hg4	159 - 343	19.52	0.05	185	1	5	30	1	6	31
ISO-hg3	344 - 408	380.71	0.13	65	41	3	49	40	3	48
ISO-hg1	409 - 620	114.72	0.04	212	32	14	65	32	14	70
ISO-s3	621 - 688	52.12	0.12	68	1	9	19	1	9	18
ISO-s2	689 - 741	127.46	0.16	53	3	7	28	2	7	26
ISO-s1	742 - 804	198.68	0.13	63	5	7	11	4	7	10
ISO-base	805 - 1099	99.07	0.03	295	10	30	112	6	35	112
Total	1 - 1099	115.16	0.06	1099	99	80	339	89	87	343

Figure 23: Effect of Weighting Factors: Optimal Layering Distribution of Amellago with No Cutoff

Zones	Layers	PermX (mD)	Average Porosity	Number of fine layers	Number of Coarse Layers					
					Net Rock Volume Weighted			Pore Volume Weighted		
					With Cutoff			With Cutoff		
					Velocity	Slowness	VS	Velocity	Slowness	VS
ISO-s4	1 - 158	139.27	0.06	158	5	2	4	3	3	12
ISO-hg4	159 - 343	19.52	0.05	185	1	48	72	1	34	72
ISO-hg3	344 - 408	380.71	0.13	65	41	27	38	40	31	50
ISO-hg1	409 - 620	114.72	0.04	212	32	94	136	32	95	153
ISO-s3	621 - 688	52.12	0.12	68	1	24	1	1	48	8
ISO-s2	689 - 741	127.46	0.16	53	3	1	4	2	18	6
ISO-s1	742 - 804	198.68	0.13	63	5	38	50	4	35	50
ISO-base	805 - 1099	99.07	0.03	295	9	59	63	6	106	161
Total	1 - 1099	115.16	0.06	1099	97	293	368	89	370	512

Figure 24: Effect of Weighting Factors: Optimal Layering Distribution of Amellago With Cutoff

However, interestingly enough when the two factors of cutoffs and weighting factors are imposed together, we observe major changes and improvement in the layering scheme. Figure 25 shows how the individual zonal layering as also the total layering count for coarse models have significantly changed from the base case (net rock volume weighted + no cutoffs). This is also manifested in the heterogeneity plots where we notice the combination of cutoffs and introduction of a new weighting factor helped reduce the apparent preservation of heterogeneity.

Zones	Layers	PermX (mD)	Average Porosity	Number of fine layers	Number of Coarse Layers					
					Net Rock Volume Weighted			Pore Volume Weighted		
					No Cutoff			With Cutoff		
					Velocity	Slowness	VS	Velocity	Slowness	VS
ISO-s4	1 - 158	139.27	0.06	158	6	5	25	3	3	12
ISO-hg4	159 - 343	19.52	0.05	185	1	5	30	1	34	72
ISO-hg3	344 - 408	380.71	0.13	65	41	3	49	40	31	50
ISO-hg1	409 - 620	114.72	0.04	212	32	14	65	32	95	153
ISO-s3	621 - 688	52.12	0.12	68	1	9	19	1	48	8
ISO-s2	689 - 741	127.46	0.16	53	3	7	28	2	18	6
ISO-s1	742 - 804	198.68	0.13	63	5	7	11	4	35	50
ISO-base	805 - 1099	99.07	0.03	295	10	30	112	6	106	161
Total	1 - 1099	115.16	0.06	1099	99	80	339	89	370	512

Figure 25: Effect of Cutoffs + Weighting Factors: Optimal Layering Distribution of Amellago

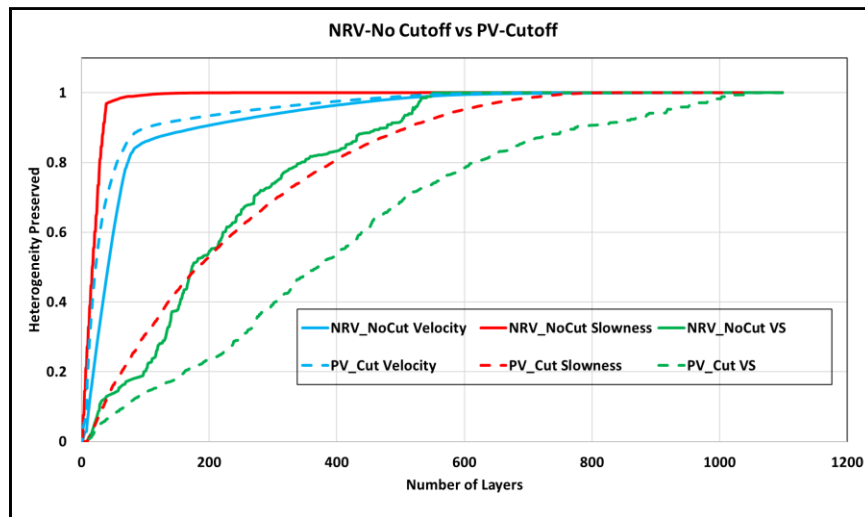


Figure 26: Effect of Cutoffs + Weighting Factors: Heterogeneity Plot

Improved Upgridding: Zonal Averaging and Zonal Upgridding

In our existing SWIFT calculations, we have been computing the average for properties along the entire length of each column in the grid. In doing so, we calculate the variance of the cells of all zones about one particular mean for each column. This calculation of variance is however not an accurate representation of the statistical error measures capturing the heterogeneity distribution throughout the model. The mean property is observed to be more closely related as a property characteristic to a particular zone, instead of the entire model (which consists of multiple zones). This technique has been named as ‘Zonal Averaging’.

The following set of equations would help us discuss how SWIFT has been modified to incorporate ‘Zonal Averaging’.

Previously, the averaged property was calculated based on Eqn. (19). Now, we calculate the average corresponding to every zone, as follows:

$$\bar{P}_{ij,zone} = \frac{\sum_{k=1}^{NZ,zone} n_{ijk} P_{ijk}}{\sum_{k=1}^{NZ,zone} n_{ijk}} \dots\dots\dots (30)$$

The rest of the equations remain the same as the existing SWIFT calculations.

We also attempted to formulate a new measure for combining ‘Velocity’ and ‘Slowness’. Currently, our combination of the two error measures involved calculating the RMS of the error measures at the cellular level. However, that led to more jagged and uneven curves, often leading to non-monotonicity. Instead, we formulated a new method of computing the combination error by taking the RMS of the ‘Velocity’ and ‘Slowness’ error measures

over the entire model, and named it as ‘RMS(V+S)’. This has significantly improved the smoothness of the heterogeneity curves as also minimized the collapse of fine scale layers into very low number of coarse layers.

Formulation of equations for RMS(V+S):

We calculate the ‘Velocity’ error as:

$$E_V = \sum_{i,j,k}^{NX,NY,NZ} (V^C - \bar{V})^2 \dots\dots\dots (31)$$

Similarly, we calculate the ‘Slowness’ error as:

$$E_S = \sum_{i,j,k}^{NX,NY,NZ} (S^C - \bar{S})^2 \dots\dots\dots (32)$$

RMS(V+S) error was calculated as:

$$E_{RMS} = \sqrt{E_V E_S} \dots\dots\dots (33)$$

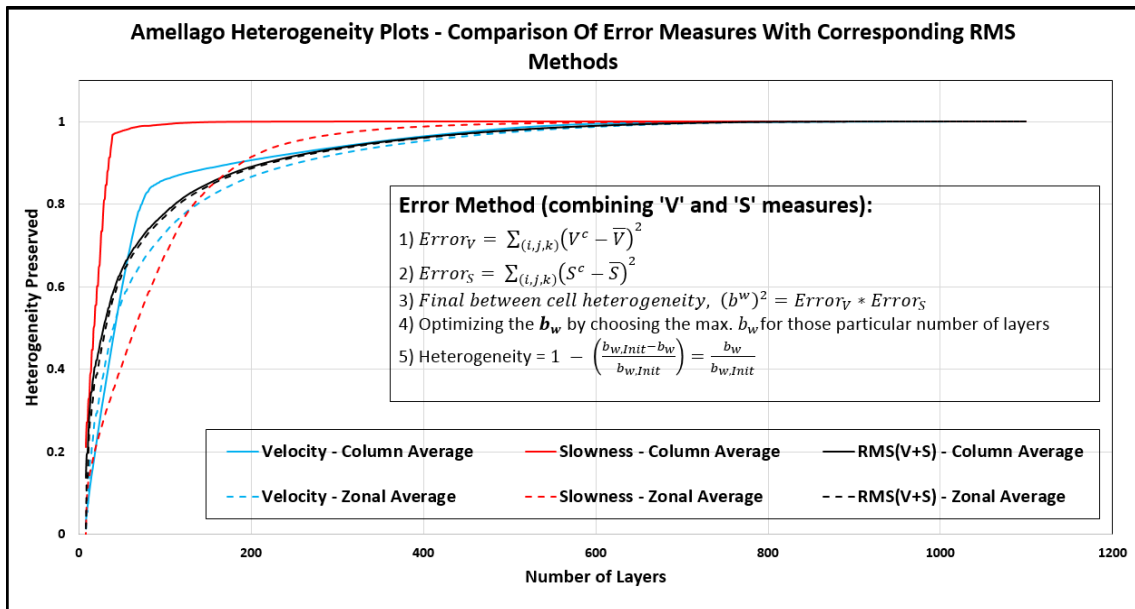


Figure 27: Upgridding Heterogeneity Plot for Amellago: Column Averaging vs Zonal Averaging

Zones	Layers	Number of fine layers	Number of coarse layers					
			Column Average			Zonal Average		
			Velocity	Slowness	RMS	Velocity	Slowness	RMS
ISO-s4	1 - 158	158	3	6	24	25	2	25
ISO-hg4	159 - 343	185	1	6	52	52	15	52
ISO-hg3	344 - 408	65	40	3	20	20	22	20
ISO-hg1	409 - 620	212	32	14	42	42	37	42
ISO-s3	621 - 688	68	1	9	3	3	10	3
ISO-s2	689 - 741	53	2	7	10	10	5	10
ISO-s1	742 - 804	63	4	7	8	8	1	8
ISO-base	805 - 1099	295	6	35	25	25	109	25
Total	1 - 1099	1099	89	87	184	185	201	185

Figure 28: Effect of Averaging on the Optimal Layering Distribution for Amellago

Figure 28 represents a comparative study of the layering scheme after coarsening of Amellago model using both prior-art column averaging method and the new Zonal averaging method. We observe that, Zonal Averaging preserves more layers per zones as compared to the previous methods for the same error measure. However, it is surprising to notice how the layering schemes for RMS(V+S) error measure remains almost unchanged for both the methods.

The reason RMS(V+S) was introduced is to compute the combination of the error of the two variances on a full-model scale, rather than on a cell-by-cell scale.

Table 10 compares the optimal number of layers from both methods. It is noticed how RMS(V+S) method biases around the Velocity measure more than Slowness.

Previously we looked into how the different zones behaved with respect to each other in terms of the number of layers contained per zone. We also take a look into the layering

distributions within the zones, i.e. number of fine layers contained in each coarse layer for each error measure.

Table 10 - Effect of Averaging Method on Optimal Layer Count for Amellago

Optimal Layer Counts			
Error Measures	Column Average	Zonal Average	Average Layer Count
Velocity	89	185	137
Slowness	87	201	144
RMS (V+S)	184	185	185

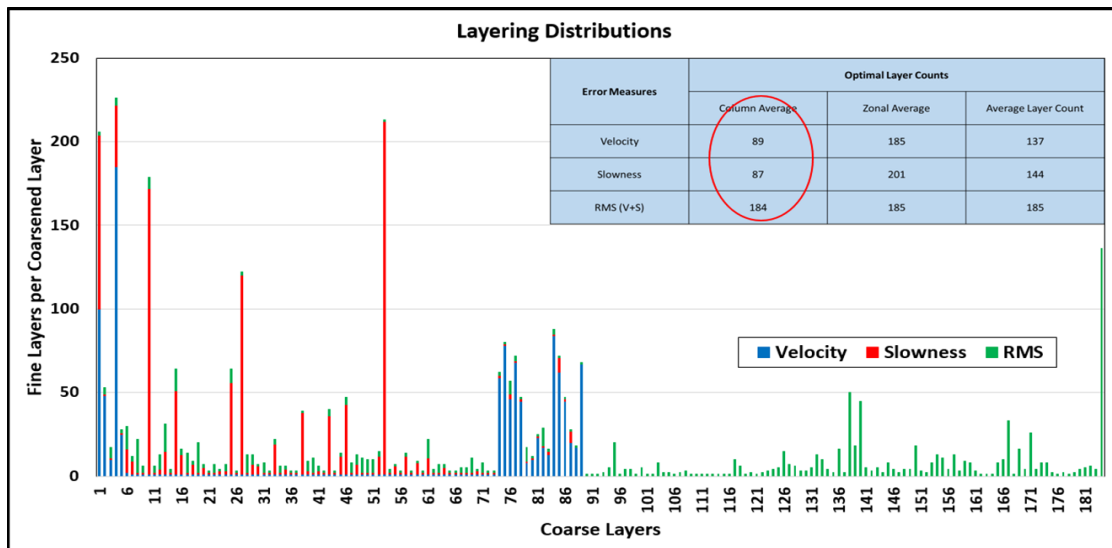


Figure 29: Layering Distribution of Amellago using Column Averaging Method

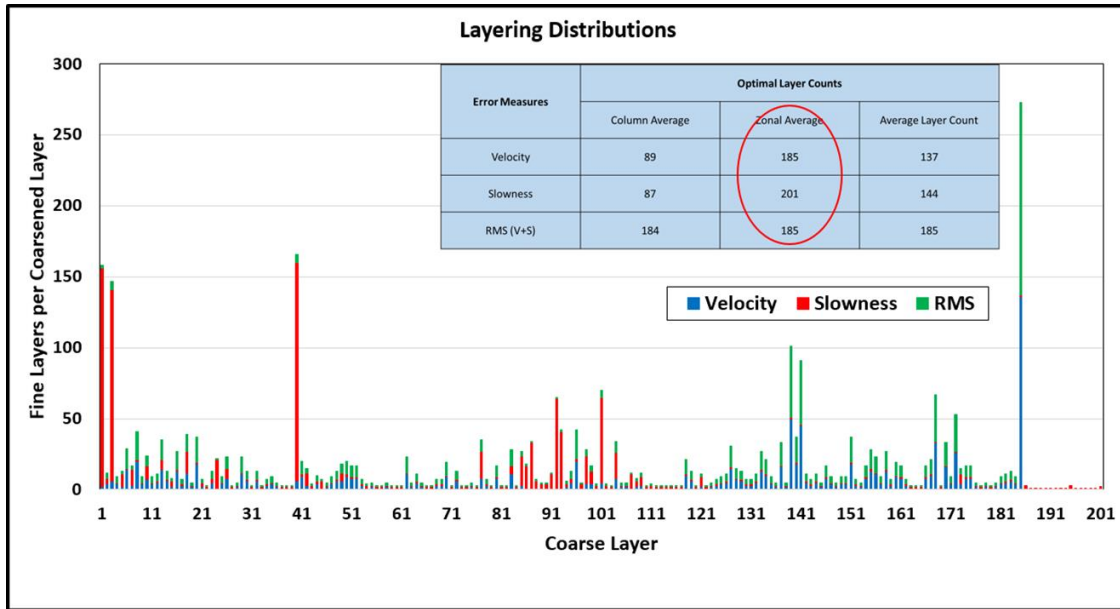


Figure 30: Optimal Layering Distribution of Amellago using Zonal Averaging Method

However, while we were probing into the effects of Zonal Averaging, we realized that we still calculate the total Heterogeneity of the entire model for layer grouping. However, in order to preserve the characteristic differences of the different zones, we need to calculate the total heterogeneity of each zone separately. This led to the formulation of ‘Zonal Upgridding’, where we treat every zone as independent individual model and we coarsen them optimally. Upon completion of coarsening the zones individually, we stack the layering schemes of the zones in order to get the optimal layering scheme of the entire model.

Here we would go through the equations involved in ‘Zonal Upgridding’:

We start with Eqn. (30). However, the calculation of B and W are for each zone now, as opposed to for the entire model before.

Therefore, we have:

$$B_{zone} = H(P_{zone}^C) = \sum_{i,j,k=1}^{(NX,NY,NZ)_{zone}} n_{ijk} (P_{ijk}^C - \bar{P}_{ij})^2 \dots\dots\dots (34)$$

$$\delta B_{zone} = - \sum_{i,j}^{(NX,NY)_{zone}} \frac{n_{ijk_1} n_{ijk_2}}{n_{ijk_1} + n_{ijk_2}} (P_{ijk_1}^C - P_{ijk_2}^C)^2 \dots\dots\dots (35)$$

We still follow Eqn. (26) and merge layers based on δW_{zone} . Based on Eqns. (34) and (35)

we can also formulate VS error measure as:

$$\delta W_{VS_{zone}} = \sum_{i,j}^{(NX,NY)_{zone}} \sum_{k=k_1,k_2} n_{ijk} \left| \left(V_{ijk} - \frac{\bar{k}_{ij_{zone}}}{\bar{\phi}_{ij_{zone}}} \right) \left(S_{ijk} - \frac{\bar{\phi}_{ij_{zone}}}{\bar{k}_{ij_{zone}}} \right) \right| \dots\dots\dots (36)$$

Heterogeneity present in that particular zonal model is calculated as:

$$B_{VS_{zone}} = \sum_{i,j,k=1}^{(NX,NY,NZ)_{zone}} n_{ijk} \left| \left(V_{ijk} - \frac{\bar{k}_{ij_{zone}}}{\bar{\phi}_{ij_{zone}}} \right) \left(S_{ijk} - \frac{\bar{\phi}_{ij_{zone}}}{\bar{k}_{ij_{zone}}} \right) \right| \dots\dots\dots (37)$$

- **Change of weights for ‘Zonal Upgridding’:**

Our previous attempts at accurately quantifying the weighting factors involved changing the weights from net rock volume to pore volume. However, we would look more closely at the following table and notice that porosity is not the only criteria that controls the spatial distribution of heterogeneity. Porosity and Permeability are both important and hence should be considered into the calculations. In Figure 31, zone 3 shows somewhat evenly distributed high values of bulk volume (net volume equals the bulk volume since

net-to-gross is not defined for this model) throughout the map. However, the porosity and permeability maps actually show that only certain channelized patches are high quality and those are the ones that contribute to the fluid flow.

Accordingly, the weighting factor chosen is:

$$W.F. = \sqrt{\bar{k}\bar{\phi}}V_n \dots\dots\dots (38)$$

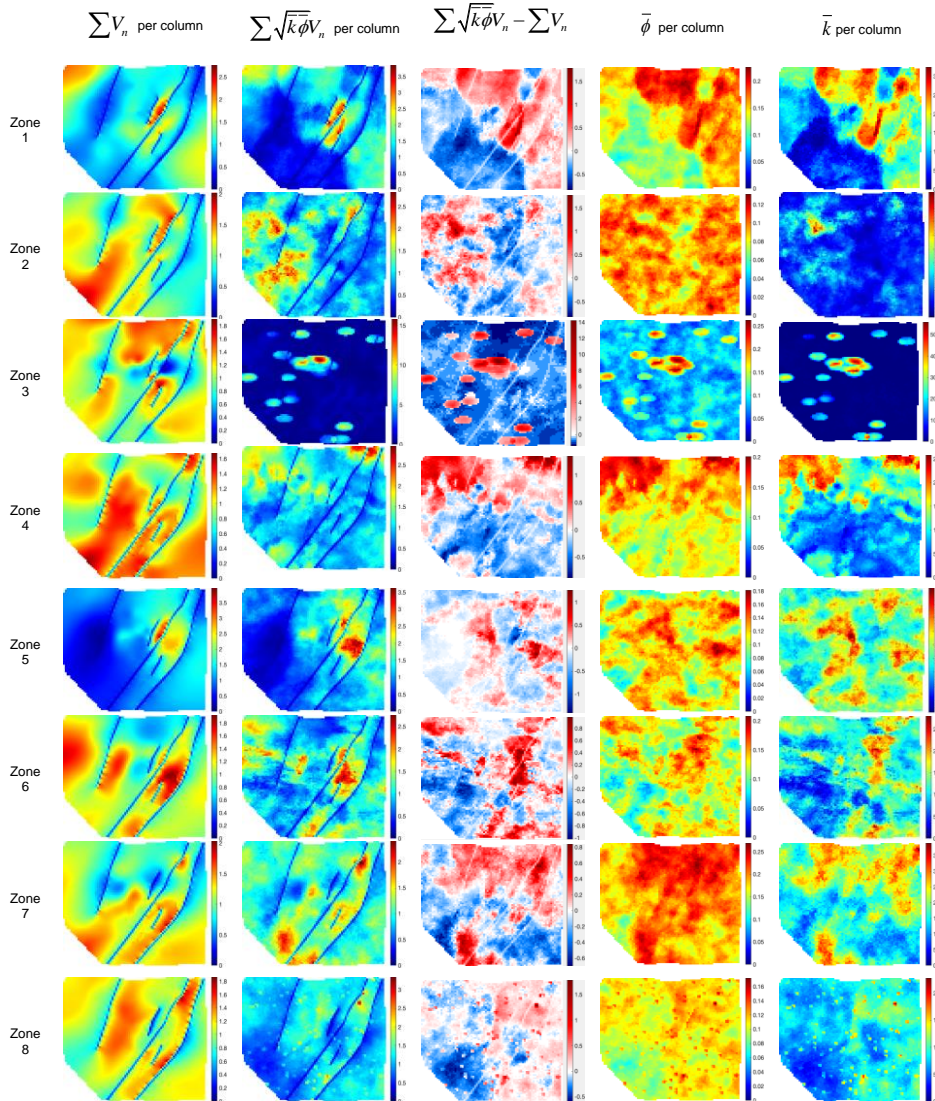


Figure 31: 2D Map View of Different Properties of Amellago Model (Liu, 2019)

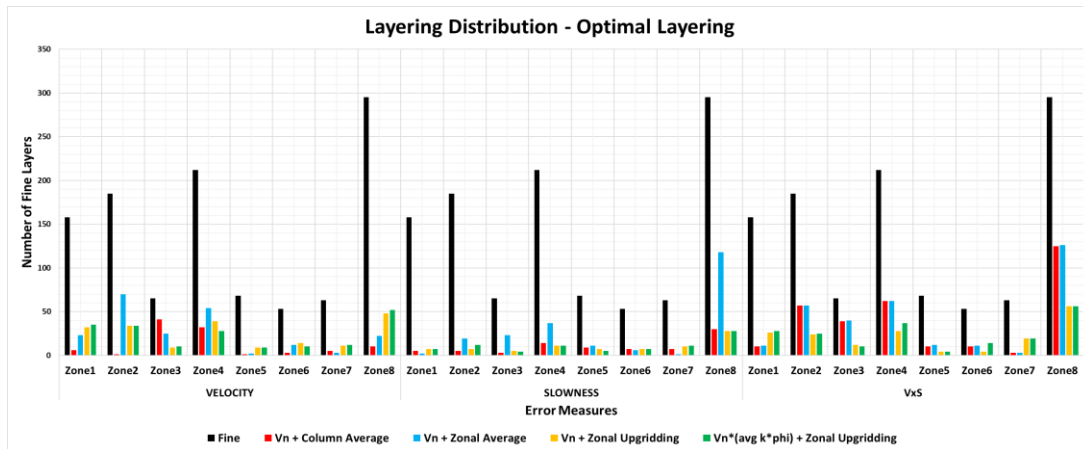


Figure 32: Optimal Layering Distribution for Amellago: Comparison of Zonal Upgridding vs Other Methods

Figure 32 represents the layering distribution for Amellago for different averaging techniques. We observe how zonal averaging preserves a greater number of layers (under optimal conditions) compared to column averaging methods, for every error measure.

Changing the weighting factor from V_n to $\sqrt{k\bar{\phi}}V_n$ shows slight difference in the layering scheme.

Figure 33 shows the heterogeneity plot comparing zonal averaging with the existing column averaging methods. As we introduce averaging based on zones, the curves shift more towards the x-axis, i.e. they do not remain as aggressive as they did previously.

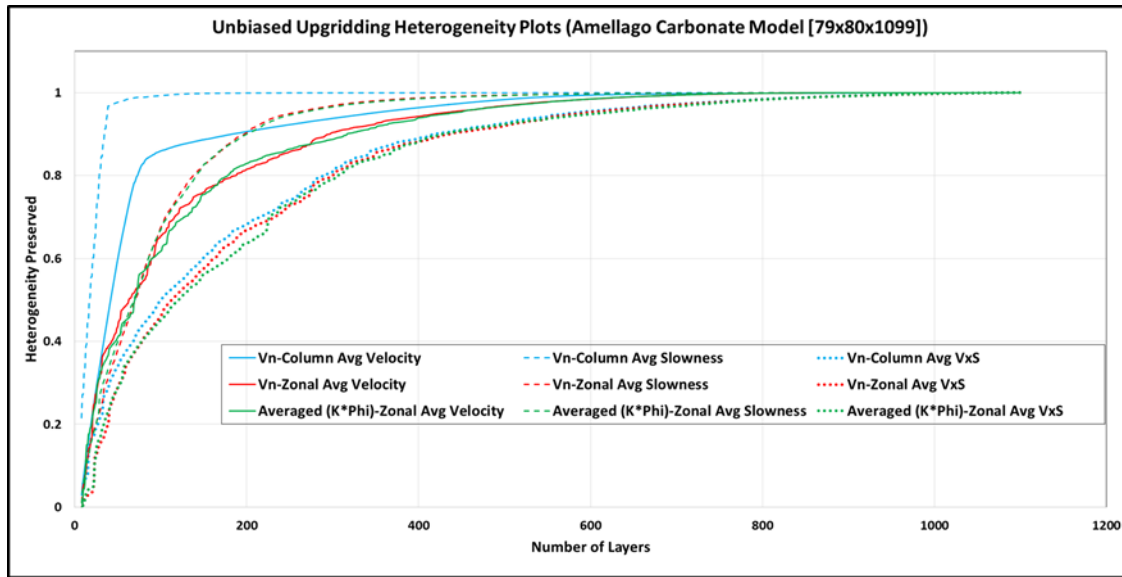


Figure 33: Upgridding Heterogeneity Plot for Amellago: Comparison of Zonal Averaging

Results of the ‘Zonal Upgridding’ analysis for Amellago are shown in Figure 34 (Liu, 2019). Each zone is designed independently of the others and all three error measures are shown. Each point on the curve is in some sense, an optimal layer design, as it is chosen to maximize a measure of the heterogeneity preserved in the coarsened model. For each measure, it is seen that the variance is largely preserved until a certain degree of coarsening is reached and after which the heterogeneity decreases rapidly with further layer coarsening. This cross-over point on each curve defines the optimal number of layers for each zone. Interestingly, for the Amellago model, the optimal number of layers does not

vary significantly with the choice of error measure and indicates a conservative coarsening ratio of approximately x6 for each measure.

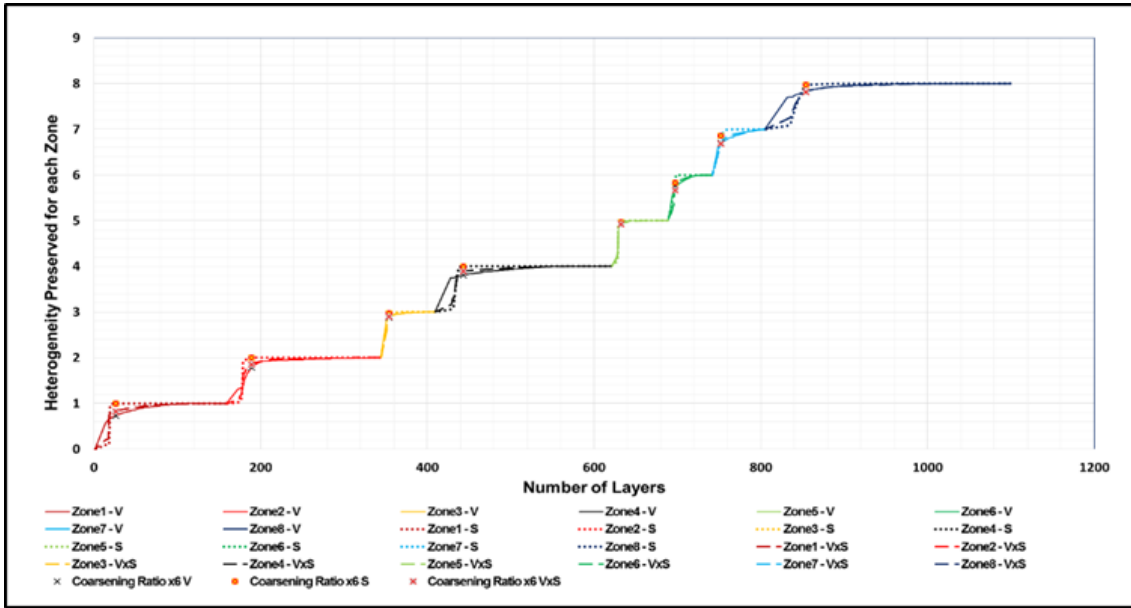


Figure 34: Amellago Zonal Layer Design Heterogeneity Plot (Three Heterogeneity Measures) (Liu, 2019)

Figure 35 tabulates a comparison of the advanced zonal upgridding layering scheme with the results from the existing upgridding algorithms. We notice how the collapse of fine layers and apparent preservation of heterogeneity have been minimized. Coarsening ratios of 185 have been reduced to only 5, i.e. more fidelity have been preserved in the model for that particular zone.

Zones	PermX	Average Porosity	Fine Layers	Number of Fine Layers	Coarsening Ratios (Optimal Number of Layers)					
					Vn-Column Avg			Zonal Upgridding		
					Velocity	Slowness	VxS	Velocity	Slowness	VxS
ISO-s4	139.27	0.06	1 - 158	158	26	32	40	5	8	6
ISO-hg4	19.52	0.05	159 - 343	185	185	37	9	5	7	5
ISO-hg3	380.71	0.13	344 - 408	65	2	22	2	7	7	7
ISO-hg1	114.72	0.04	409 - 620	212	7	15	6	7	7	7
ISO-s3	52.12	0.12	621 - 688	68	68	8	34	7	6	7
ISO-s2	127.46	0.16	689 - 741	53	18	8	53	5	5	4
ISO-s1	198.68	0.13	742 - 804	63	13	9	32	5	4	5
ISO-base	99.07	0.03	805 - 1099	295	30	10	3	5	6	5
Total	115.16	0.06	1 - 1099	1099	11	14	6	5	6	6

Figure 35: Comparison of Optimal Layering Distribution for Amellago: Zonal Averaging vs. Zonal Upgridding

- **Flow Simulation Results: Single Phase Simulation:**
 - 5 producers @ 160 bar BHP
 - 4 injectors in the center @ 240 bar BHP [Oil Injection]
 - Simulation time: 1 year
 - Oil single phase
 - ECLIPSE Transmissibility Upscaling + Steady State Algebraic Well Index Upscaling

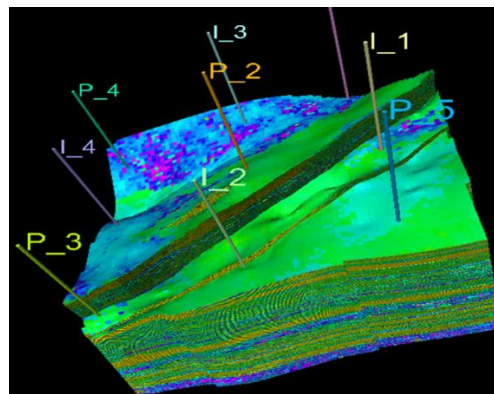


Figure 36: Amellago 3D Model: Well Locations for Flow Simulation

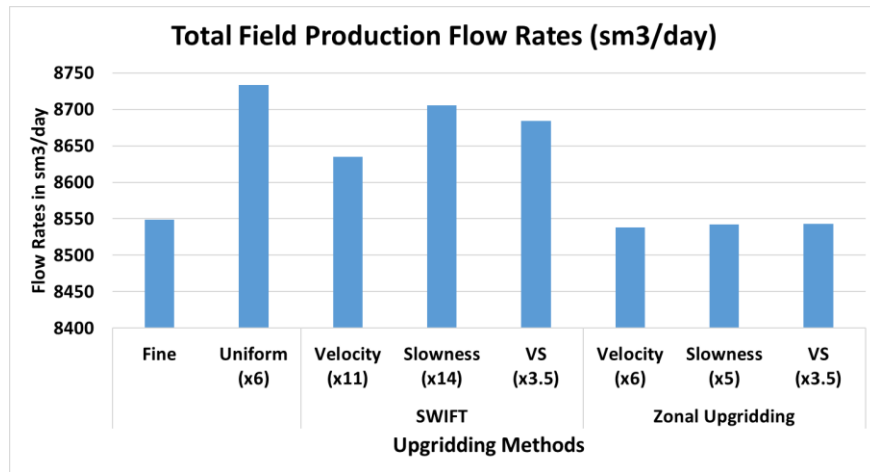


Figure 37: Total Production Flow Rates Comparison for Amellago

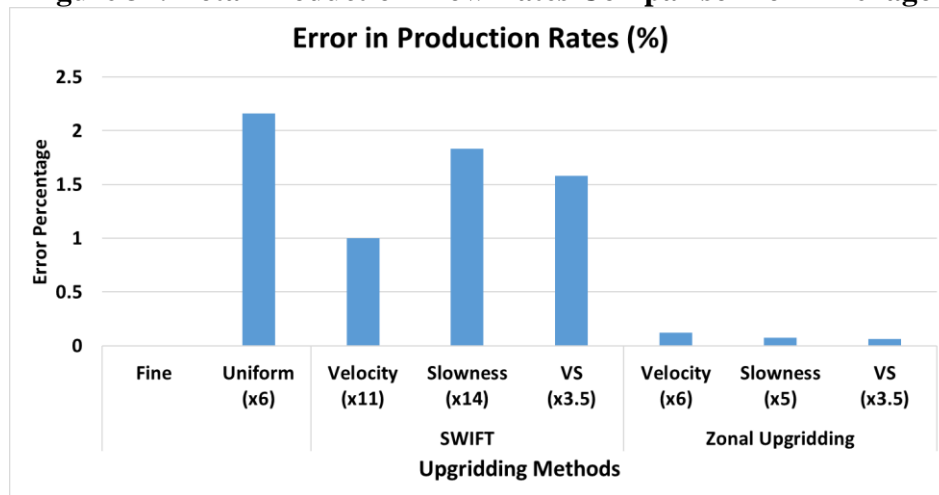


Figure 38: L2 Norm Errors for Well Rates for Amellago

Figure 37 and Figure 38 depict how close the coarsened model flow simulation results are with the fine scale model. Thus, we have successfully been able to preserve the flow characteristics of the fine scale model as much as possible while reducing the cell count by a factor of 6. Error measures of <0.5% are observed when using Zonal Upgridding as opposed to errors >1.5%, which is a great improvement.

However, this improvement comes at a price. As mentioned earlier, Zonal Upgridding treats every zone separately as an independent model and performs coarsening. This is a rather cumbersome procedure, time consuming and less economic. Also, evaluation of averages per zone makes the task less efficient.

Apart from the other major problems that our existing algorithm already had, we attempt to make improvements to Upgridding even further. Hence, this paved the way for a robust, very efficient, recursive, practical technique for upgridding. This is dealt in details in the next chapter on “Distance Based Upgridding”.

CHAPTER IV

DISTANCE BASED UPGRIDDING

Theoretical Background

The new sequential layer coarsening technique is based on a concept of model distance. In the coarsening sequence, each model is chosen to be as close as possible to the previous model. Thereby, we calculate the difference between two sequential models instead of calculating the total heterogeneity as a variance for each column.

For the unbiased variance, “Within” cell heterogeneity is calculated according to Eqn. (25) Again, this follows the usage of Testerman (1962). This equation can be interpreted as a measure of distance between two sequentially coarsened models, rather than a calculation of a variance around a specific mean.

From the above equation, the model distance is defined as follows when merging layers k_1 and k_2 :

$$\delta W = \sum_{i,j,k} \delta W_{i,j,k} = \sum_{i,j,k=1}^{NX,NY,NZ} n_{ijk} (P_{ijk} - P_{ijk}^C)^2 = \sum_{i,j} \sum_{k=k_1,k_2}^{NX,NY} n_{ijk} (P_{ijk} - P_{ijk}^C)^2 \dots\dots\dots (39)$$

We now start from this relationship to obtain a more general distance measure.

$$\delta W = \sum_{i,j=1}^{NX,NY} \sum_{k=l_1,l_2} \phi_{ijk} k_{ijk} n_{ijk} |(V_{ijk} - V_{ijk}^C)(S_{ijk} - S_{ijk}^C)| \dots\dots\dots (40)$$

For the pair of layers k_1 and k_2 , we define V_{ijk}^C and S_{ijk}^C as follows:

$$V_{ijk}^C = \frac{k_{ijk}^C}{\phi_{ijk}^C} \text{ and } S_{ijk}^C = \frac{\phi_{ijk}^C}{k_{ijk}^C} \dots\dots\dots (41)$$

In addition, instead of defining the heterogeneity using the explicit form of Eqn. (25), we now define it implicitly by:

$$\delta W = -\delta B \dots\dots\dots (42)$$

This ensures that the quantity used to identify the layers for sequential coarsening is also used as a measure of the model heterogeneity.

Novelty: How novel is this method?

This method is inherently different from the previous sequential layering algorithm.

- 1) We do not need to base our calculations on pre-defined mean values of properties for each column. According to Eqn. (19), a volume weighted average velocity or slowness needed to be calculated which is essentially a pure statistical estimate. Cumulative sum of δW_{\min} at every step of coarsening now replaces the equations for B (Eqns. (22) and (28)).
- 2) Using physical properties that arise in the coarsened models at different resolutions while coarsening, i.e., V^C and S^C instead of \bar{V} and \bar{S} (Eqn. (19)) provides a more rational physical quantity to work with and use as a representation of model heterogeneity.
- 3) We know, $\delta W = -\delta B = \sum_{i,j,k} (P_{ijk} - P_{ijk}^C)^2$. Therefore, we notice that the variance error from Eqn. (23) has been replaced by the distance measure.
- 4) Also, the new choice of weights ensures that the heterogeneity measures are correctly estimated. As shown earlier, net rock volume over-estimates the variance

calculation. So proper weights make sure variance values are not absurdly high or low. From Eqn. (40), we see that the new choice of weights is $\phi_{ijk} k_{ijk} n_{ijk}$

Testing Distance Based Upgridding on SPE10

We have performed our novel Distance based upgridding on SPE10 model and the results are shown in the later section of this chapter. Before we get to the results, we would do a brief characterization of the SPE10 model.

- **SPE10 Model Characterization**

SPE10 is a simple sandstone geologic model. It has simple geometry, with no top surfaces or faults. It is described on a regular cartesian grid. The model dimensions are 60 x 220 x 85 (1,122,000 cells).

The model consists of a part of a Brent sequence and is characterized by two formations. The first in the top 35 layers represents the Tarbert formation which is a representation of a pro-grading near shore environment. It is a low contrast, high permeability stratified sand structure. The second geologic unit is the bottom 50 layers which is a part of the Upper Ness sequence and represents fluvial environment. It consists of high permeability channels embedded in a background of low permeability. SPE10 is particularly challenging for many simulators because of its strong variations in heterogeneity in permeability.

- **Upgridding and Flow Simulation Results**

- 1. Layering Scheme:**

Zones	Fine Layers	Number of Layers								
		Fine Scale	Velocity		Slowness		VS		Distance-VxS	
			Layers	Coarsening Ratio	Layers	Coarsening Ratio	Layers	Coarsening Ratio	Layers	Coarsening Ratio
Tarbert	1-35	35	1	35	1	35	1	35	11	3.2
Upper Ness	36-85	50	14	3.6	35	1.4	18	2.8	16	3.1

Figure 39: SPE10 Layering Scheme

We observe that the Distance based upgridding method preserves resolution in both the zones and prevents collapse of fine layers, as encountered before in the prior art methods. Collapse of all 35 fine layers into 1 coarse layer (from top zone) is removed. Coarsening ratios of 3.2 and 3.1 for Distance based approach look more reasonable and pragmatic compared to absurdly high and low ratios like 35 and 1.4 respectively.

- 2. Diagnostic Plots:**

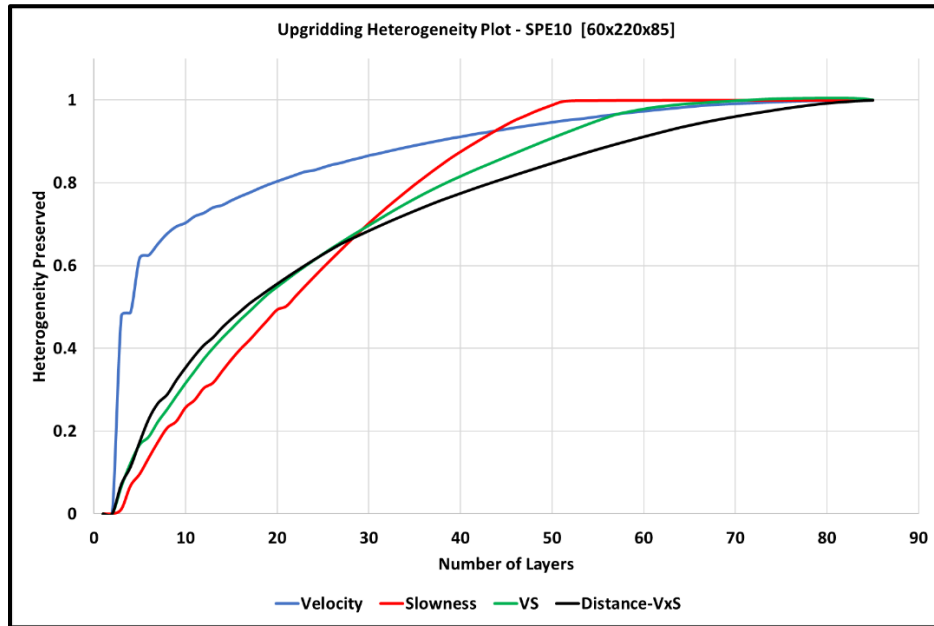


Figure 40: SPE10 Upgridding Heterogeneity Plot

Addressing another limitation of the previous methods, we observe there that for Distance based upgridding, the heterogeneity preservation shows a marked deviation from 100% as we merge layers, unlike apparent preservation of almost 100% heterogeneity even at very low layers.

3. Single Phase Simulation: We have performed single phase simulation on SPE10 and the specifications for the procedure are as follows:

- 4 producers at the 4 corners @ 1000 psi BHP
- 1 injector in the center @ 4000 psi BHP [Oil Injection]
- Simulation time: 1 year
- Oil single phase.
- Steady State Transmissibility Upscaling (ECLIPSE)

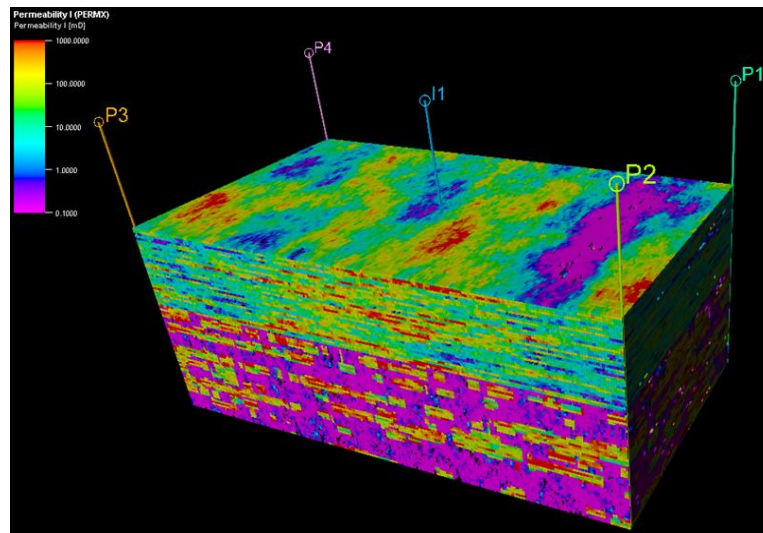


Figure 41: SPE10 3D Model: Well Locations for Flow Simulation

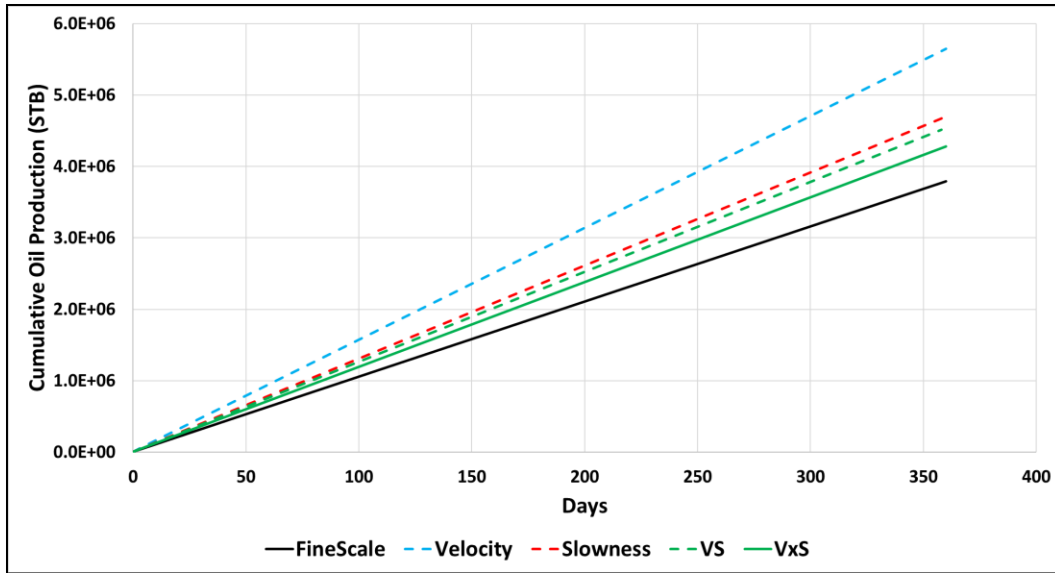


Figure 42: SPE10 Single Phase: Cumulative Oil Production

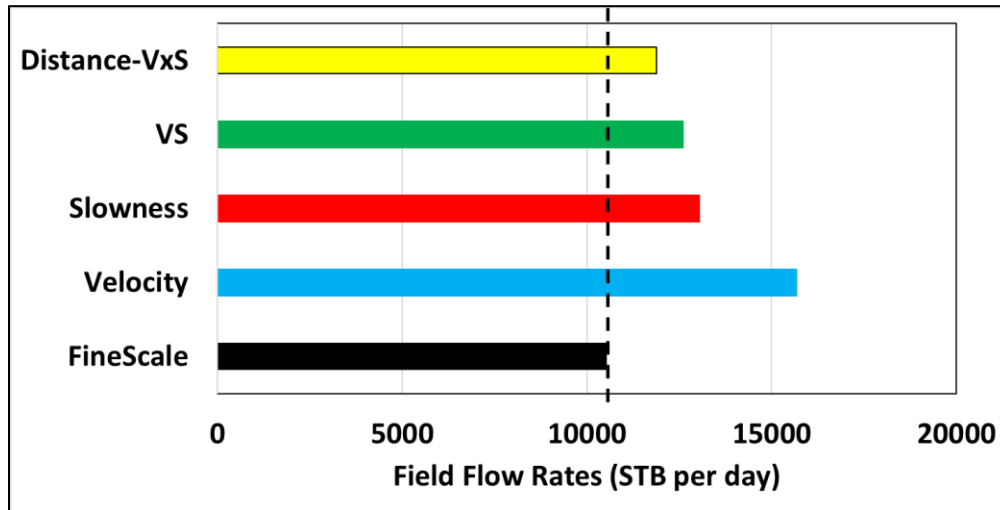


Figure 43: SPE10 Single Phase: Field Flow Rate

Figure 42 and Figure 43 depict the cumulative oil production and the field flow rates for all the existing upgridding techniques and for the novel Distance based upgridding. We can observe the Distance based method works better than the rest.

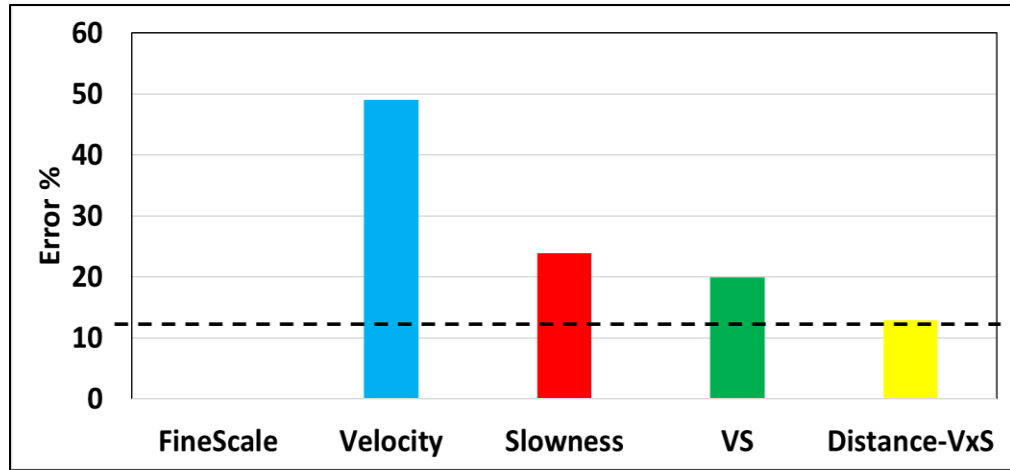


Figure 44: SPE10 Single Phase: Field Flow Rate Errors

Figure 44 shows that among all the cases, the Distance based VxS method shows closest resemblance with the fine scale model in terms of simulated results.

Testing Distance Based Upgridding on Amellago Model

1) Layering Scheme

Zones	PermX (mD)	Average Porosity	Fine Layers	Layers					Coarsening Ratios			
				Fine Scale	Vn-Column Avg			Distance Based Upgridding	Vn-Column Avg			Distance Based Upgridding
					Velocity	Slowness	VS	VxS	Velocity	Slowness	VS	VxS
ISO-s4	139.27	0.06	1 - 158	158	6	5	25	33	26.3	31.6	6.3	4.8
ISO-hg4	19.52	0.05	159 - 343	185	1	5	30	10	185.0	37.0	6.2	18.5
ISO-hg3	380.71	0.13	344 - 408	65	41	3	49	13	1.6	21.7	1.3	5.0
ISO-hg1	114.72	0.04	409 - 620	212	32	14	65	29	6.6	15.1	3.3	7.3
ISO-s3	52.12	0.12	621 - 688	68	1	9	19	5	68.0	7.6	3.6	13.6
ISO-s2	127.46	0.16	689 - 741	53	3	7	28	12	17.7	7.6	1.9	4.4
ISO-s1	198.68	0.13	742 - 804	63	5	7	11	17	12.6	9.0	5.7	3.7
ISO-base	99.07	0.03	805 - 1099	295	10	30	112	43	29.5	9.8	2.6	6.9
Total				1099	99	80	339	162				

Figure 45: Amellago Layering Scheme

Once again, the collapse of fine scale layers is minimized by the Distance based approach even for the Amellago model. All zones seem to well preserved in resolution by our new technique. This can be seen from Figure 46 above.

Diagnostic Plot

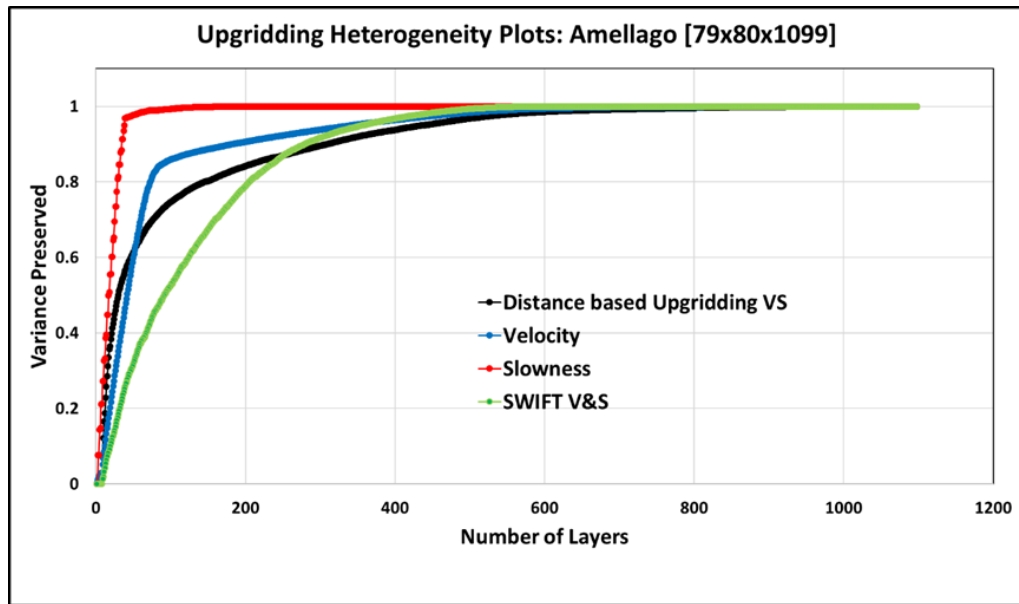


Figure 46 Amellago Upgridding Heterogeneity Plot

While the previous methods show a very high preservation of heterogeneity at low layers, VxS Distance based measure prohibits such preservation of apparent heterogeneity at higher degrees of coarsening.

2) Flow Simulation Results: Single Phase Simulation:

- 5 producers @ 160 bar BHP
- 4 injectors in the center @ 240 bar BHP [Oil Injection]
- Simulation time: 1 year
- Oil single phase
- Steady State Transmissibility Upscaling (ECLIPSE)

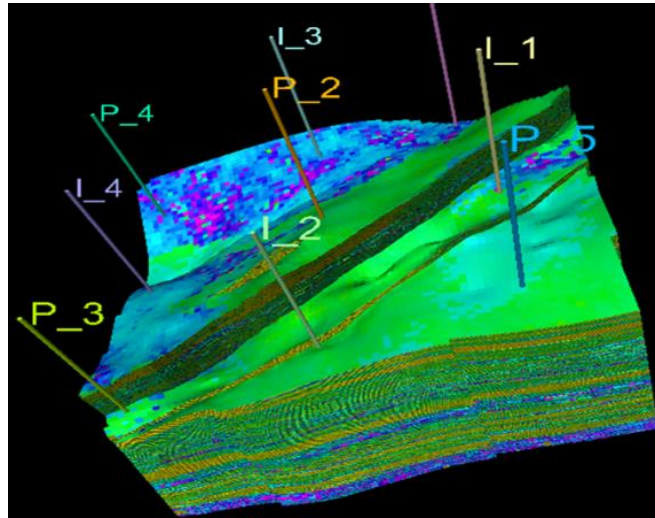


Figure 47: Amellago 3D Model: Well Locations for Flow Simulation

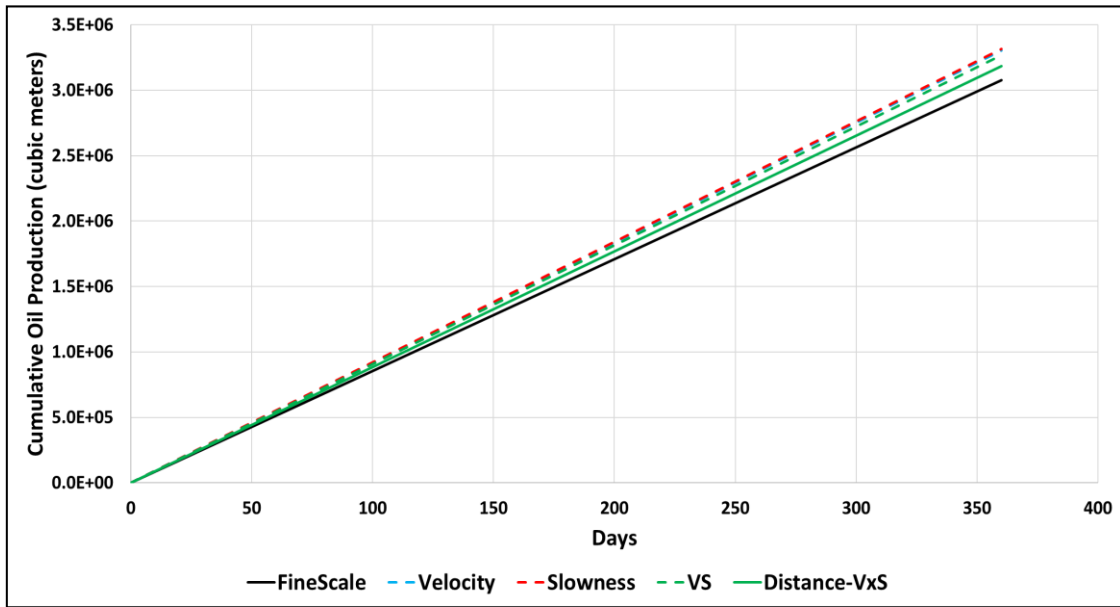


Figure 48 Amellago Simulation Results: Cumulative Oil Production

The Distance based method exhibits better results compared to the previous variance-based error upgridding techniques. This is also evident in the subsequent figures, Figure 49 and Figure 50.

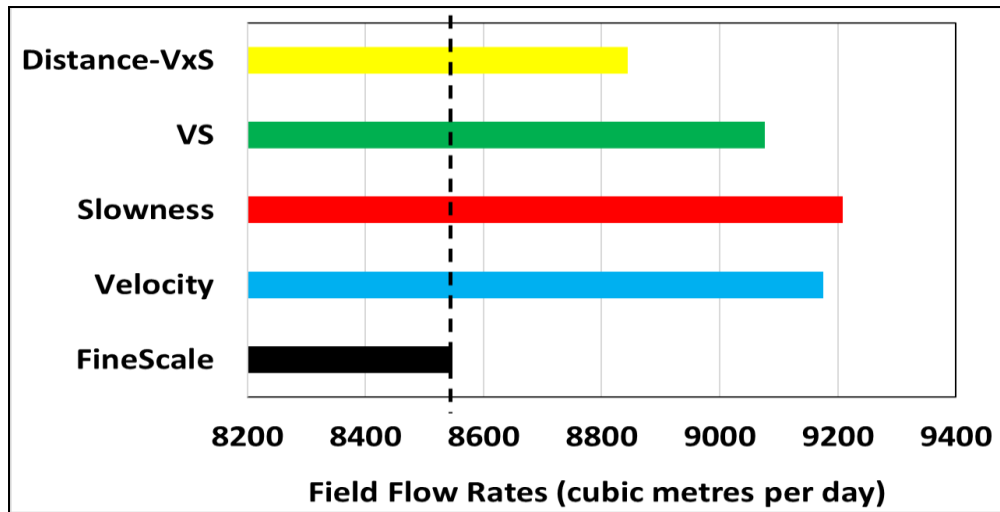


Figure 49 Amellago Simulation Results: Field Flow Rates

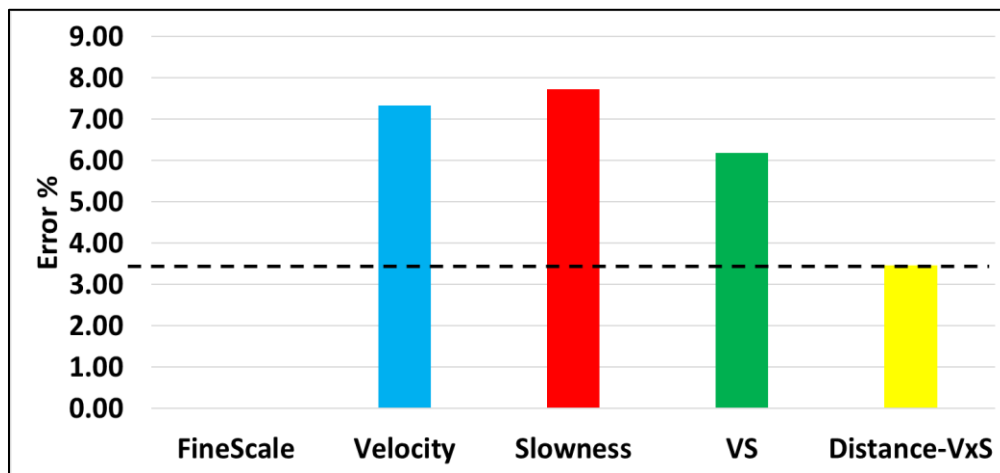


Figure 50 Amellago Simulation Results: Field Flow Rates Errors

CHAPTER V
DISCUSSIONS

Advantages

The advantages of using this novel technique over the previous SWIFT implementation are as follows:

- The new distance-based method to calculate error measures guarantees monotonicity in the quantification of heterogeneity as the models are coarsened (heterogeneity decreases upon coarsening).

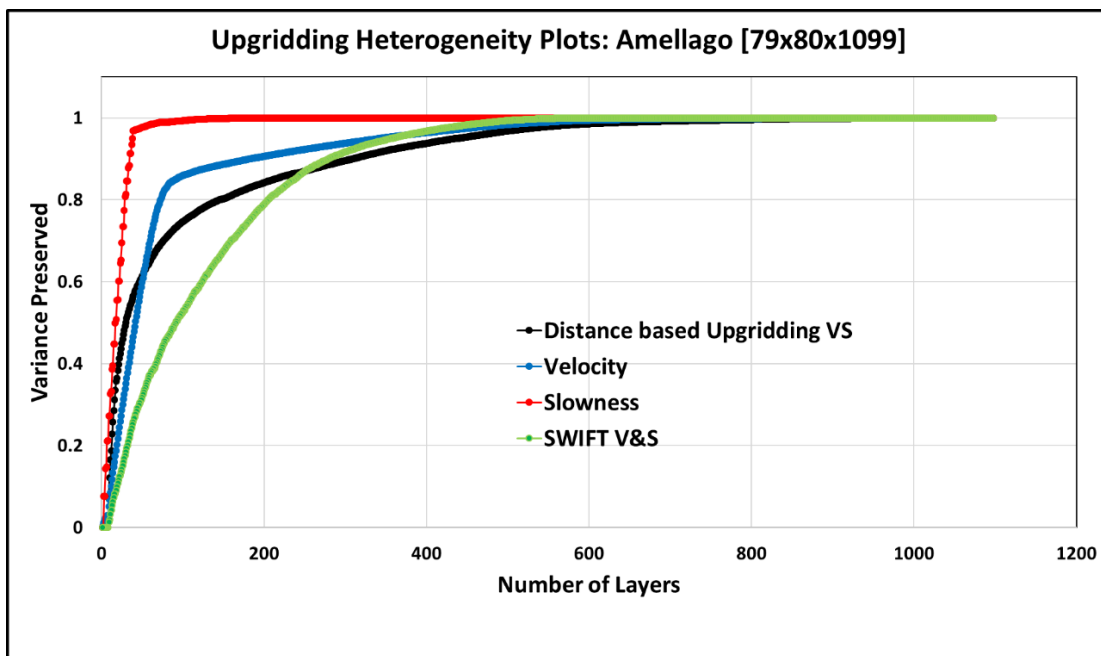


Figure 51 Distance Based VxS Heterogeneity Plot Compared with SWIFT Heterogeneity Plots

- Collapse of fine layers observed in Figure 13 is now minimized owing to monotonic and less aggressive heterogeneity plot seen in Figure 12. The high values of coarsening

ratios from SWIFT upgridding cases seen in the figure below have been mostly reduced to pragmatic values, especially for high quality zones.

Zones	Fine Scale	Vn-Column Avg						Distance Based Upgridding	
		Velocity		Slowness		VS		VxS	
		Layers	Coarsening Ratio	Layers	Coarsening Ratio	Layers	Coarsening Ratio	Layers	Coarsening Ratio
ISO-s4	158	6	26.3	5	31.6	25	6.3	33	4.8
ISO-hg4	185	1	185.0	5	37.0	30	6.2	10	18.5
ISO-hg3	65	41	1.6	3	21.7	49	1.3	13	5.0
ISO-hg1	212	32	6.6	14	15.1	65	3.3	29	7.3
ISO-s3	68	1	68.0	9	7.6	19	3.6	5	13.6
ISO-s2	53	3	17.7	7	7.6	28	1.9	12	4.4
ISO-s1	63	5	12.6	7	9.0	11	5.7	17	3.7
ISO-base	295	10	29.5	30	9.8	112	2.6	43	6.9
Total	1099	99		80		339		162	

Figure 52 Layering Scheme for Amellago model comparison: Distance Based VxS vs SWIFT algorithms

- Heterogeneity measure can be generalized now to include both Velocity and Slowness. This provides a consistent means to assess the sequencing of coarsened reservoir models for simultaneous parameters and with physically based property coarsening, thereby removing the restriction of only using a single reservoir parameter or restricting the coarsening of that parameter based on a statistically averaged value. For example, in models with X & Y anisotropy, horizontal permeability will differ along the X and Y directions. Therefore we may now use multiple data types of Velocity (V_x and V_y) and Slowness (S_x and S_y), which can be included in a totality combined error measure.
- Weights are now calculated based on permeability and porosity. Figure 31 illustrates how widely the properties (permeability and porosity) are distributed across the different zones in the model. Incorporating permeability and porosity along with volumes in the weighting factors enhances capturing the spatial distribution of heterogeneity across all zones (geologic units).

- Now, there is no need to separate the zones for calculation of averages or for coarsening as a whole. Similarly, the use of physical quantities is a better choice.

Summary

Therefore, to summarize:

- Our existing upgridding algorithm had issues that needed to be resolved
- Combination of the choice of cutoffs, weighting factors and proper averaging techniques have proven to be successful in preservation of the flow characteristic of the fine grid
- Novel Distance-Based Upgridding conceptualizes model distance in sequential layering instead of variance calculation

CHAPTER VI

CONCLUSIONS

We began with the prior art techniques to coarsen the high-resolution fine scale geologic grids and encountered several conceptual and practical problems. We listed the problems as the motivation to our research and began probing into the physics and mathematics of upgridding.

One of the breakthroughs achieved is through the development and implementation of Distance-based Upgridding. We discussed the theory and implemented it on multiple models. In all the cases, we obtained better results compared to the previous methods. We have been successfully able to preserve the optimum resolution of the model (depicted in the layering schemes and diagnostic plots) and also the fidelity of the model (simulation result comparison with fine scale model). For the best results, Distance based upgridding with VxS error measure would be recommended to follow.

Additionally, during the development of Distance based upgridding techniques, we have also researched into different variations of statistical measures that were already being used. This has been dealt in details in Chapter IV. Introduction of cutoffs, choice of different weighting factors and separating the coarsening algorithm for different zones independently have been some of the steps taken. We have shown the different results when each modification has been implemented. In this case, we have also confined the tests to Amellago model only.

To conclude:

- Results of Distance Based Upgridding is better than our existing upgridding techniques
 - Problems encountered in the existing upgridding techniques have been successfully resolved
 - Apparent preservation of heterogeneity has been minimized
 - Collapse of fine layers into coarse model has been minimized
 - Choice of weighting factor represents spatial distribution of heterogeneity much better
 - Flow simulation results for Distance Based Upgridding resembles closest to the fine scale model
- Implementing more advanced upscaling techniques would further reduce error % from flow simulation results

REFERENCES

- Durlafsky, L. J., Behrens, R. A., Jones, R. C. et al. 1996. Scale Up of Heterogeneous Three Dimensional Reservoir Descriptions. *SPE Journal* **1** (03): 313-326. <https://doi.org/10.2118/30709-PA>.
- Fincham, A. E., Christensen, J. R., Barker, J. W. et al. 2004. Up-Gridding from Geological Model to Simulation Model: Review, Applications and Limitations. Presented at the SPE Annual Technical Conference and Exhibition, Houston, Texas. 2004/1/1/. <https://doi.org/10.2118/90921-MS>.
- Hosseini, Seyyed Abolfazi and Kelkar, Mohan Gajanan. 2008. Analytical Upgridding Method To Preserve Dynamic Flow Behavior. Presented at the SPE Annual Technical Conference and Exhibition, Denver, Colorado, USA. 2008/1/1/. <https://doi.org/10.2118/116113-MS>.
- Hosseini, Seyyed Abolfazl and Kelkar, Mohan. 2010. Analytical Upgridding Method To Preserve Dynamic Flow Behavior. *SPE Reservoir Evaluation & Engineering* **13** (03): 473-484. <https://doi.org/10.2118/116113-PA>.
- Kim, Jong Uk and Datta-Gupta, Akhil. 2009. A Dual Scale Approach to Production Data Integration into High Resolution Geologic Models. Presented at the SPE Reservoir Simulation Symposium, The Woodlands, Texas. 2009/1/1/. <https://doi.org/10.2118/118950-MS>.
- King, Michael J., Burn, Karam S., Wang, Pengju et al. 2006. Optimal Coarsening of 3D Reservoir Models for Flow Simulation. *SPE Reservoir Evaluation & Engineering* **9** (04): 317-334. <https://doi.org/10.2118/95759-PA>.

- Li, D. and Beckner, B. 2000. Optimal Uplayering for Scaleup of Multimillion-Cell Geologic Models. Presented at the SPE Annual Technical Conference and Exhibition, Dallas, Texas. 2000/1/1/. <https://doi.org/10.2118/62927-MS>.
- Li, D., Cullick, A. S., and Lake, L. W. 1996. Scale-Up Of Reservoir Model Relative Permeability Using A Global Method. *SPE Reservoir Engineering* **11** (03): 149-157. <https://doi.org/10.2118/29872-PA>.
- Liu, C.-H., Nunna, K., Syed, I., & King, M. J. (2019, June 3). Evaluation of Upscaling Approaches for the Amellago Carbonate Outcrop Model. Society of Petroleum Engineers. doi:10.2118/195560-MS
- Nunna, Krishna and King, Michael J. 2020. Dynamic Diffuse-Source Upscaling in High-Contrast Systems. *SPE Journal* **25** (01): 347-368. <https://doi.org/10.2118/182689-PA>.
- Roxar. 2012. *RMS User Guide*. Stavanger, Norway: Roxar Software Solutions.
- Stern, D. and Dawson, A. G. 1999. A Technique for Generating Reservoir Simulation Grids to Preserve Geologic Heterogeneity. Presented at the SPE Reservoir Simulation Symposium, Houston, Texas. 1999/1/1/. <https://doi.org/10.2118/51942-MS>.
- Testerman, J. D. 1962. A Statistical Reservoir-Zonation Technique. *Journal of Petroleum Technology* **14** (08): 889-893. <https://doi.org/10.2118/286-PA>.
- Zhou, Yijie and King, Michael J. 2011. Improved Upscaling for Flow Simulation of Tight Gas Reservoir Models. Presented at the SPE Annual Technical Conference and

Exhibition, Denver, Colorado, USA. 2011/1/1/. <https://doi.org/10.2118/147355->

[MS.](#)